

# Beyond Euclid:

## An Illustrated Guide to Modern Machine Learning with Geometric, Topological, and Algebraic Structures

Sophia Sanborn\*<sup>1</sup> Johan Mathe\*<sup>2</sup> Mathilde Papillon\*<sup>1</sup> Domas Buracas<sup>3</sup> Hansen J Lillemark<sup>3</sup>  
Christian Shewmake<sup>3,5</sup> Abby Bertics<sup>1</sup> Xavier Pennec<sup>4</sup> Nina Miolane<sup>1,2,3</sup>

<sup>1</sup>University of California, Santa Barbara   <sup>2</sup>Atmo, Inc.   <sup>3</sup>New Theory AI   <sup>4</sup>Université Côte d’Azur & Inria  
<sup>5</sup>University of California, Berkeley

**Abstract**—The enduring legacy of Euclidean geometry underpins classical machine learning, which, for decades, has been primarily developed for data lying in Euclidean space. Yet, modern machine learning increasingly encounters richly structured data that is inherently non-Euclidean. This data can exhibit intricate geometric, topological and algebraic structure: from the geometry of the curvature of space-time, to topologically complex interactions between neurons in the brain, to the algebraic transformations describing symmetries of physical systems. Extracting knowledge from such non-Euclidean data necessitates a broader mathematical perspective. Echoing the 19th-century revolutions that gave rise to non-Euclidean geometry, an emerging line of research is redefining modern machine learning with non-Euclidean structures. Its goal: generalizing classical methods to unconventional data types with geometry, topology, and algebra. In this review, we provide an accessible gateway to this fast-growing field and propose a graphical taxonomy that integrates recent advances into an intuitive unified framework. We subsequently extract insights into current challenges and highlight exciting opportunities for future development in this field.

**Index Terms**—Geometric Deep Learning, Geometry, Topology, Algebra, Machine Learning

### I. INTRODUCTION

For nearly two millennia, Euclid’s *Elements of Geometry* formed the backbone of our understanding of space and shape. This ‘Euclidean’ view of geometry—characterized by flat planes and straight lines—remained unquestioned until the 19th century. Only then, did mathematicians venture “beyond” to develop the principles of non-Euclidean geometry on curved spaces. Their pioneering work revealed that there is no singular, true geometry. Instead, Euclidean geometry is but one in a mathematical universe of geometries, each of which can be used to illuminate different structures in nature—from the mechanics of celestial bodies embracing the curvature of spacetime to the topologically and algebraically complex electri-

cal patterns of neurons in natural and artificial neural networks.

This non-Euclidean revolution was part of a greater trend towards generalization and abstraction in 19th and 20th century mathematics. In addition to expanding the realm of *geometry*, mathematicians proceeded to define more abstract notions of space, freed from rigid geometric concepts like distances and angles. This gave rise to the field of *topology*, which examines the properties of a space that are preserved under continuous transformations such as stretching and bending. By abstracting away from the rigidity of geometric structures, topology emphasizes more general spatial properties such as continuity and connectedness. Indeed, two structures that look very different from a geometric perspective may be considered topologically equivalent. The famous of example of this is a donut and coffee mug, which are topologically equivalent since one can be continuously deformed into the other. This notion of abstract equivalence was supported by the simultaneous development of the field of abstract *algebra*, which examines the symmetries of an object—the transformations that leave its fundamental structure unchanged. These mathematical ideas quickly found applications in the natural sciences, and revolutionized how we model the world.

A similar revolution is now unfolding in machine learning. In the last two decades, a burgeoning body of research has expanded the horizons of machine learning, moving beyond the flat, Euclidean spaces traditionally used in data analysis to embrace the rich variety of structures offered by non-Euclidean geometry, topology, and abstract algebra. This movement includes the generalization of classical statistical theory and machine learning in the field of *Geometric Statistics* (Guigui et al., 2023, Pennec, 2006) as well as deep learning models in the fields of *Geometric*, (Bron-

stein et al., 2021), *Topological* (Bodnar, 2023, Hajij et al., 2023a), and *Equivariant* (Cohen et al., 2021) *Deep Learning*. In the 20th century, non-Euclidean geometry radically transformed how we model the world with pen and paper. In the 21st century, it is poised to revolutionize how we model the world with machines.

This review article provides an accessible introduction to the core concepts underlying this movement. We organize the models in this body of literature into a coherent taxonomy defined by the mathematical structure of both the *data* and the machine learning *model*. In so doing, we clarify distinctions between approaches and we highlight challenges and high-potential areas of research that are as-of-yet unexplored. We begin by introducing the essential mathematical background in Section II, and turn to an analysis of mathematical structure in data in Section III before introducing our ontology of machine learning and deep learning methods in Section IV and V. We explore the associated landscape of open-source software libraries in Section VI, and delve into the movement’s key application domains in Section VII. Accordingly, this review article reveals how this new framework for machine learning—born from the elegant mathematics of geometry, topology, and algebra—has been developed, implemented, and adapted to propose transformative solutions to real-world challenges.

#### Topological Properties

- Connectedness      • Continuity
- Relationships

#### Geometric Properties

- Distance              • Angle
- Measurements

#### Algebraic Properties

- Symmetry              • Invariance
- Transformations

## II. ELEMENTS OF NON-EUCLIDEAN GEOMETRY

We first provide an accessible and concise introduction to the essential mathematical concepts. For readability, we define the concepts primarily linguistically here, and refer the reader to the works Bronstein et al. (2021), Cohen et al. (2021), Guigui et al. (2023), Hajij et al. (2023a) for their precise mathematical definitions.

*Topology, geometry* and *algebra* are branches of mathematics that study the properties of abstract spaces. In machine learning, data can possess explicit spatial structure—such as an image of a brain scan, or a rendering of a protein surface. Even when data is not overtly spatial, a dataset can be naturally conceptualized as a set of samples drawn from an abstract surface embedded in a high-dimensional space. Understanding the “shape” of data—that is, the shape of the space to which this data belongs—can give important insights into the patterns of relationships that give data its meaning.

Topology, geometry and algebra each provide a different lens and set of tools for studying the properties of data spaces and their “shapes,” summarized in the textbox below. **Topology** lends the most abstract, flexible perspective and considers spaces as stretchy structures that can be continuously deformed so long as *connectivity* and *continuity* are preserved. Topology thus studies the *relationships* between points. **Geometry** allows us to quantify familiar properties such as *distances* and *angles*, in other words: perform *measurements* on points. **Algebra** provides the tools to study the *symmetries* of an object—the transformations that can be applied while leaving its fundamental structure invariant.

### A. Topology: Relationships

A **topological space** is a set of points equipped with a structure known as a *topology* that establishes which points in the set are “close” to each other. The topology gives spatial structure to an otherwise unstructured set. Formally, a topology is defined as a collection of **open sets**. An open set is a collection of points in a spatial region that excludes points on the boundary. By grouping points into open sets, we can discuss ‘neighborhoods’ of points and ‘paths’ between points, giving us a way to formalize concepts like continuity (can you travel from one location to another without teleporting?) and connectedness (are two locations in the same neighborhood or region?).

Given the generality of topological structures, topological spaces can be quite exotic. Within this paper, we do not consider continuous topological spaces, and we explicitly restrict the term **topology** to **discrete topological structures**, such as graphs, cellular complexes, and hypergraphs. We consider these spaces to be a generalization of the discretized Euclidean space. Indeed, Euclidean space discretizes into a regular grid, while graphs, cellular complexes and hypergraphs relax the regularity assumption and allow points to be con-

nected with more complex relationships as illustrated in Figure

### B. Geometry: Measurements

A **manifold** is a continuous space that locally “resembles” (is homeomorphic to) Euclidean space in the neighborhood of every point. In other words, it is locally linear, and it does not intersect itself. Though locally it resembles flat space, its global shape may exhibit curvature. Without additional structure, the manifold can be seen as a soft and elastic surface. To give it more rigid, definite form, a manifold can be equipped with a notion of *distance* between points, that freezes how far each point is from each other, and therefore freezes the overall shape of the manifold.

There are two main approaches to defining a distance on the manifold, which turn it into either (i) a metric space, where an extrinsic distance may be chosen independently of the manifold’s properties, or into (ii) a length space (also called path-metric spaces), where the **distance** between two points on the manifold is defined intrinsically by the infimum of the length of curves connecting the points. Within this paper, we focus on length spaces. A powerful way of establishing a notion of distance for this approach is to consider a **Riemannian manifold**, that is: a smooth manifold equipped with a positive definite inner product on the tangent space at every point on the manifold. This family of inner products defines the **Riemannian metric**, which defines the lengths of tangent vectors at a given point on the manifold and the angle between them. Ultimately, the Riemannian metric induces a distance along a curve of the manifold through integration of its tangent vector. A **geodesic** generalizes the Euclidean concept of a “straight line” to curved manifolds. A Riemannian geodesic is a curve that traces the locally shortest path between two points.

There exist different flavors of Riemannian manifolds, such as the spheres, hyperbolic spaces, and tori. We consider these spaces to be generalizations of the continuous Euclidean space. Indeed, Euclidean spaces are globally flat, while spheres, hyperbolic spaces and tori can exhibit curvature—as illustrated in Figure 2. It is no coincidence that the manifolds most commonly studied in the literature—the Euclidean space, the hypersphere, and the hyperbolic space—are the three manifolds of constant curvature. The Euclidean space has curvature 0, the sphere (and hyperspheres) have curvature 1, while the hyperbolic spaces have curvature -1. The uniformity of their curvature makes

them simpler to model than more general, arbitrary manifolds.

### C. Algebra: Transformations

A **group** is a set of transformations, such as 3D rotations, that can be composed. Groups can be discrete or continuous. A **Lie group** is a continuous group, defined as a smooth manifold equipped with a compatible group structure such that the composition of elements on the manifold obeys the group axioms. An example of a Lie group is the set of special orthogonal matrices in  $\mathbb{R}^{3 \times 3}$  under matrix multiplication, which defines the group of 3-dimensional rotations,  $SO(3)$ . Each matrix is an element of the group and defines rotation at a certain angle. Lie groups are extensively used in physics where they describe symmetries in physical systems.

A group of transformations, such as  $SO(3)$ —the group of 3D rotations—may act on another manifold to transform its elements. A **group action** maps an element in a manifold to new location, determined by the group element that transforms them. For example, a group action on a Euclidean space can translate, rotate and reflect its elements, as illustrated in Figure 3. In this paper, we use the term **algebra** to denote that we equip a space with a **group action**.

## III. STRUCTURE IN DATA

The mathematics of topology, geometry and algebra provide a conceptual framework to categorize the nature of data found in machine learning. We generally encounter two types of data: either data as *coordinates in space*—for example the coordinate of the position of an object in a 2D space; or data as *signals over a space*—for example, an image is a 3D (RGB) signal defined over a 2D space. In each case, the *space* can either be a Euclidean space or it can be equipped with topological, geometric and algebraic structures such as the ones introduced in Section II.

Understanding the structure of this space provides essential insights into the nature of the data. These insights are, in turn, crucial for selecting the machine learning model that will be most suitable to extract knowledge from this data. In this section, we provide a graphical taxonomy, shown in Figure 4, to categorize the structures of data based on the mathematics of topology, geometry and algebra.

### A. Data as Coordinates in Space

We start by categorizing the mathematical structures of data, when data points are *coordinates in space*—as

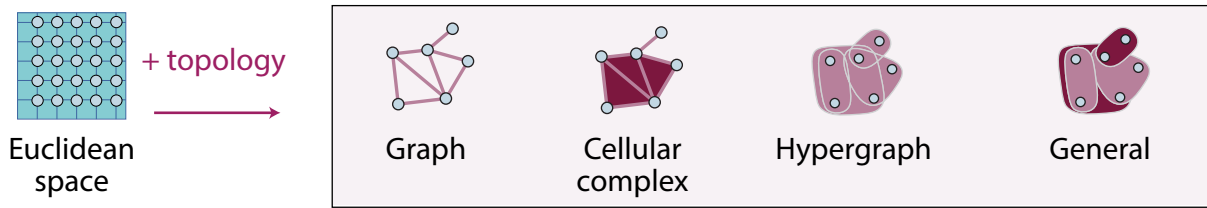


**Fig. 1: Beyond Euclid: Discrete Topological Structures.** Left: Euclidean space discretized into a regular grid. Right: Discrete topological spaces that go beyond the classical discretized Euclidean space. Graphs, Cellular Complexes, Hypergraphs relax the assumption of the regular grid and allow points to be connected with more complex relationships. The arrow `+topology` indicates the addition of a non-Euclidean, discrete topological structure. Adapted from Papillon et al. (2023).

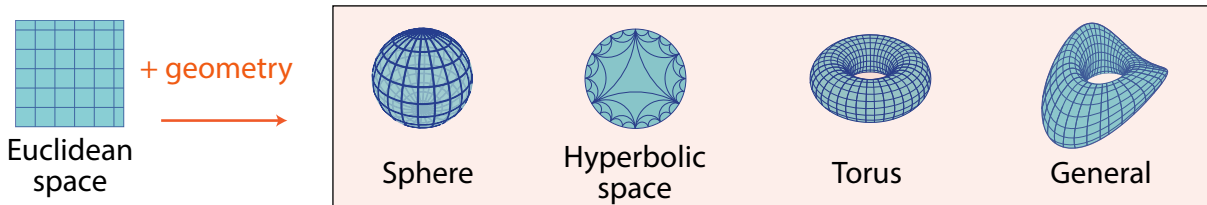


**Fig. 2: Beyond Euclid: Continuous Geometric Structures.** Left: Euclidean space. Right: Riemannian manifolds that go beyond the classical Euclidean space. Spheres, hyperbolic spaces, and tori relax the assumption of flatness of the Euclidean space and can exhibit positive or negative curvature. The arrow `+geometry` indicates the addition of a non-Euclidean, continuous geometric structure.

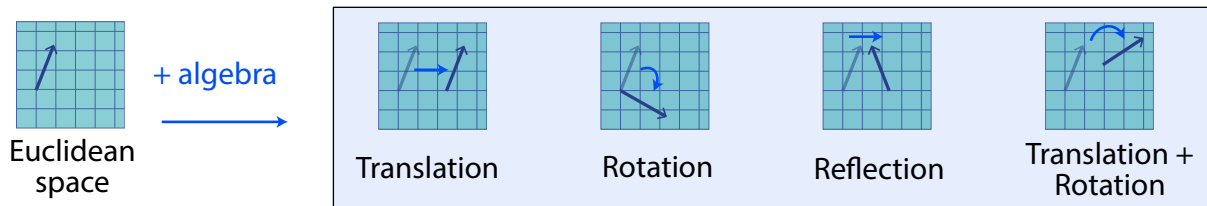


**Fig. 3: Beyond Euclid: Algebraic Transformations.** Left: Euclidean space. Right: Group transformations that act on the elements of an Euclidean space: 2D translation from the group  $\mathbb{R}^2$ , 2D rotation from the group  $SO(2)$ , 2D reflection from the group  $\{1, -1\}$ , and a combination of translation and rotation from the Special Euclidean group  $SE(2)$ . The arrow `+algebra` indicates the addition of the non-Euclidean algebraic structure defining a group action.

shown in the top two rows of Figure 4, and described in detail below. We denote with  $x$  a data point within a dataset  $x_1, \dots, x_i, \dots, x_N$ , and drop its subscript  $i$  for conciseness of notations.

**Card C1: Point in Euclidean space:** This category of data points forms the basis of conventional machine learning and deep learning approaches. Card C1 (white) in Figure 4 shows an example of a point in Euclidean space  $\mathbb{R}^n$ , which represents the dimensions of a flower from the Iris dataset (Fisher, 1936), where  $n$  represents the number of features studied.

**Card C2: Point in manifold:** Adding a non-Euclidean geometry to the coordinate space, card C2 (orange) illustrates a data point on a manifold  $M$ , where the manifold is the sphere. For example, this data point can represent

the geographic coordinates of a storm event, i.e., its location on the surface of the earth represented as a sphere.

**Card C3: Point in topological space:** Card C3 (purple) considers a data point that resides in a topological space  $\Omega$ , here corresponding to a node in a graph. An example in this category would be a data point representing a person in the graph of a social network, where edges represent social relationships.

The next three data categories add a group action to the data spaces mentioned above.

**Card C4: Point in Euclidean space equipped with group action:** Card C4 (blue) displays a data point in a Euclidean space that has been equipped with a group action. Group actions enable us to model and preserve symmetries in the data. For example, a group action on

the flower dimensions could be the change of units, from centimeters to millimeters. In this case, the group of interest is the group of scalings  $\mathbb{R}_+^*$ . The action of this group does not change the information contained in the data (the flower will still have the same size in the real world), it only changes the way we encode that information.

Card C5: **Point in manifold equipped with group action:** Card C5 adds the notion of group action to manifold. An example of such a group action could be a change of coordinate systems on the sphere, changing the origin of longitudes. In this case, the group of interest would be the group of 3D rotations  $SO(3)$ . Again, the action of this group represents symmetries in the data: the information content is unchanged (a storm will still happen at the same geographical location in the real world) but the way we encode that information has changed.

Card C6: **Point in topological space equipped with group action:** Card C6 equips a topological space with the notion of group action. An example of this is a graph of people equipped with an action that can change the way indexing is done on the dataset. The order in which we index people does not change their social relationships, only the way we represent this data in the computer. The group of interest in this case is the group of permutations.

These categories describe the *mathematical* structure of the data spaces encountered in machine learning. However, even when data points belong to spaces with topological, geometric, or algebraic structures, their *computational* representations typically take the form of arrays. These data points may thus appear as vectors in a computer’s memory, but this is merely a convenience for processing and storage. The underlying mathematical structure is preserved through constraints imposed on the values of these vectors.

For example, a data point lying on a sphere might be represented as a 3D coordinate vector, but constraints on the norm of this vector encode the properties that define the mathematical space. We note that a data point can be represented by arrays of different sizes. For example, the data point on the sphere can be represented with vector of size 3 with values encoding its Cartesian coordinates, or with a vector of size 2

with values representing its latitude and longitude. In both cases, the mathematical nature of the data point is unchanged: it still represents a point on a manifold, independently of the array used to process it in the computer.

## B. Data as Signals

In many applications, data points are not coordinates in space but rather *functions* defined over a space, typically assigning a vector in  $\mathbb{R}^{m'}$  to every point in the space  $\mathbb{R}^m$ . Formally, we can write such a function as  $x : \mathbb{R}^m \rightarrow \mathbb{R}^{m'}$  where the input space (here,  $\mathbb{R}^m$ ) is called the domain and the output space (here,  $\mathbb{R}^{m'}$ ) is called the codomain. We refer to data of this type as a **signal**. Elements of the codomain are called the values of the signal  $x$ .

Color images provide a clear example of this. The domain is a bounded region of  $\mathbb{R}^2$ : for example, limited to the range  $[0, 1920]$  on the horizontal axis and  $[0, 1080]$  on the vertical axis such that each point in the domain represents a pixel location. Each pixel location is assigned a vector in the codomain  $\mathbb{R}^3$ , which specifies the intensity on each RGB color channel.

Figure 4 introduces several types of data points as functions from a domain to a codomain, together with real-world data examples. Formalizing a signal in this way gives us the flexibility to represent more general classes of signals using non-Euclidean structures. The domain or the codomain (or both) may be any one of the non-Euclidean spaces introduced in the previous section. We present the different options in the four bottom rows of Figure 4 and detail them below.

Card S1: **Euclidean signal on Euclidean domain:** This represents one of the most common type of data in classical deep learning, functions as  $x : \mathbb{R}^m \rightarrow \mathbb{R}^{m'}$ , going from points in domain  $\mathbb{R}^m$  to features in codomain  $\mathbb{R}^{m'}$ . A gray-scale image provides a clear example of this. The domain is a bounded region of  $\mathbb{R}^2$  representing pixel locations. Each pixel location is assigned a vector in codomain  $\mathbb{R}$ , which specifies the intensity in gray scale.

Card S2: **Manifold-valued signal on Euclidean domain:** This represents signals that can be formalized as a function  $x : \mathbb{R}^m \mapsto M'$ , which assigns an element of a manifold  $M'$  to every point in the Euclidean domain  $\mathbb{R}^m$ . An example of this occurs in diffusion tensor imaging, in which 3D images of the brain are taken. Attached to each voxel location

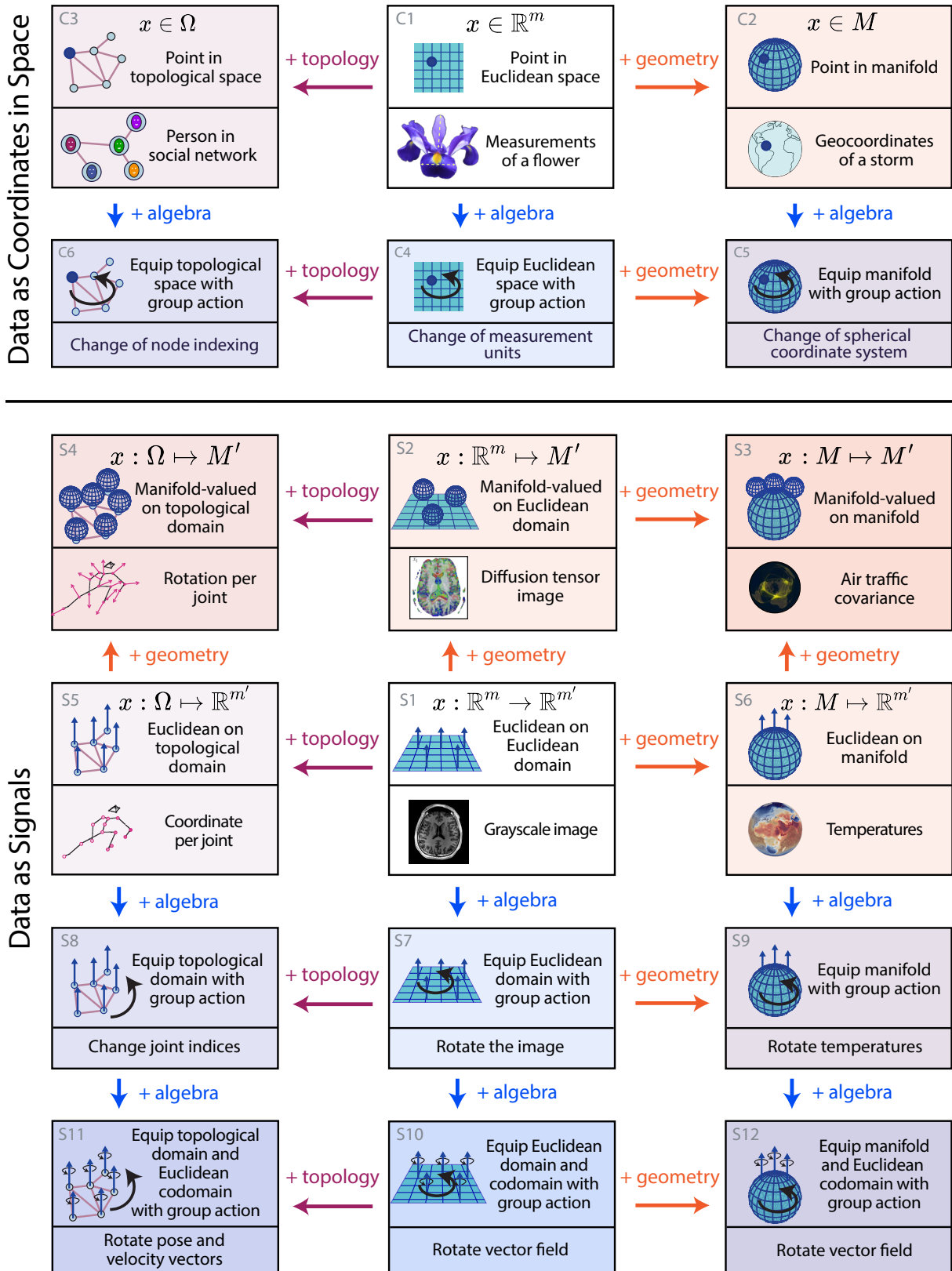


**Fig. 4: Geometric, Topological, and Algebraic Structures in Data.** We categorize data into two types: *data as coordinates* in a mathematical space (top 2 rows) or *data as signals*, i.e., as a function over a mathematical space with values in another space (bottom four rows). Each card illustrates the structure of data and presents a real-world example. The arrows + topology, + geometry and + algebra between cards indicate the addition of non-Euclidean topological, geometric and algebraic structures respectively. Notations:  $\mathbb{R}^m$ : Euclidean space of dimension  $m$ ,  $M$ : Manifold,  $\Omega$ : Topological space;  $x$ : data as point or as signal.

in domain  $\mathbb{R}^3$  is a  $3 \times 3$  covariance matrix that describes how water molecules diffuse in the brain—i.e., an element from the manifold of symmetric positive definite matrices  $M' = SPD(3)$  (Pennec et al., 2006).

- Card S3: **Manifold-valued signal on manifold domain:** In this category, both the domain and the codomain are manifolds  $M$  and  $M'$ , respectively, i.e.,  $x : M \mapsto M'$ . Air traffic covariance data is a use case where the domain is the sphere  $M = S^2$  (earth surface) and the values are  $2 \times 2$  SPD matrices, i.e., elements of the manifold codomain  $M' = SPD(2)$ . These matrices can encode covariance matrices representing different levels of local complexity (Le Brigant and Puechmorel, 2018).
- Card S4: **Manifold-valued signal on topological domain:** Here, the signal inputs live in a topological domain  $\Omega$  and the signal values live on a manifold  $M'$ , such that  $x : \Omega \mapsto M'$ . A representative example for this setting is human pose. Each joint in the body is represented by its 3D orientation, i.e., by a rotation matrix on the special orthogonal group of 3D rotations  $M' = SO(3)$ . The domain, representing the indexing of the body joints, can be encoded as a non-directed graph  $\Omega$ .
- Card S5: **Euclidean signal on topological domain:** This represents a signal with a topological domain  $\Omega$  and values in a Euclidean space  $\mathbb{R}^{m'}$ , that is:  $x : \Omega \mapsto \mathbb{R}^{m'}$ . Reusing the example of encoding the human pose, each body joint can instead be represented by its 3D location in space, i.e., with a value in  $\mathbb{R}^{m'} = \mathbb{R}^3$  defined over the non directed graph domain  $\Omega$ .
- Card S6: **Euclidean signal on manifold domain:** This represents the signal inputs on a manifold  $M$  and the signal values in Euclidean space  $\mathbb{R}^{m'}$ , i.e.,  $x : M \mapsto \mathbb{R}^{m'}$ . An example of this is a datapoint representing a snapshot of the earth at a given time showing the distribution of temperatures across the globe: the earth surface temperatures locations live on the sphere manifold  $M = S^2$  and the temperature themselves are in  $\mathbb{R}^{m'} = \mathbb{R}$  (image and dataset credits: Atmo, Inc.).
- The next categories of data structure add a group action in either the domain or the codomain (or both) of a given signal  $x$ .
- Card S7: **Euclidean signal on topological domain equipped with domain action:** The signal here is  $x : \Omega \mapsto \mathbb{R}^{m'}$ , where  $\Omega$  is equipped with a group action. An example of application here is the pose of the human body, where the domain is a undirected graph representing the body joints and the group action on the domain is the group of permutations. Permutations can re-index the order of the body joints by changing the indexing of the nodes of the graph representing the joints.
- Card S8: **Euclidean signal on manifold domain equipped with domain action:** Here, the signal is  $x : M \mapsto \mathbb{R}^{m'}$ , where the manifold domain  $M$  is equipped with a group action. Using the earth surface temperature example from Card S6, we can apply a rotation on the domain by changing the origin of the spherical coordinates for instance. In that case, the action group is the group of rotations  $SO(3)$  acting on  $M = S^2$ .
- Card S9: **Euclidean signal on Euclidean domain equipped with domain and codomain actions:** This represents signals such as  $x : \mathbb{R}^m \rightarrow \mathbb{R}^{m'}$ , where both domain  $\mathbb{R}^m$  and codomain  $\mathbb{R}^{m'}$  are equipped with group actions. The illustration in the cards shows a vector field in a domain  $\mathbb{R}^2$  with values as vectors in  $\mathbb{R}^2$ . In this example, the actions on both the domain and the codomain are from the group of rotations  $SO(2)$ , which applies the same rotation to each point in the domain and for each independent vector in the vector field.
- Card S10: **Euclidean signal on topological domain equipped with domain and codomain actions:** Here, the function is  $x : \Omega \mapsto \mathbb{R}^{m'}$ , where both  $\Omega$  and  $\mathbb{R}^{m'}$  are equipped with group actions. The permutation group acts on the domain by changing the joint indices in the graph  $\Omega$  and the 3D rotation group  $SO(3)$  acts on the values representing velocity vectors at each joint.
- Card S11: **Euclidean signal on manifold domain equipped with domain and codomain ac-**

**tions:** Here  $x : M \mapsto \mathbb{R}^{m'}$ , where both  $M$  and  $\mathbb{R}^{m'}$  are equipped with group actions. We present an example of a vector field defined over the sphere  $S^2$  with vector values in  $\mathbb{R}^{m'}$ . In this example, applying the action of a 3D rotation rotates both the spherical coordinates of the vectors and their actual vector directions. This can be useful for changes of coordinates.

As in the previous subsection, we emphasize the difference between the *mathematical* representation of data and the *computational* representation of data. Until now, we described data as signals represented as functions  $x$  over a domain. However, most of the time, the functions  $x$  are discretized in the computer. For example, the domain of a function representing a 2D color image as the signal  $x : \mathbb{R}^2 \mapsto \mathbb{R}^3$  is discretized into a grid with  $p^2$  pixels, where each pixel has a value in  $\mathbb{R}^3$ . The data point  $x$  is therefore represented, in the computer, by an array of length  $p^2 * 3$ .

A recent line of research—the literature of operators and neural operators (Kovachki et al., 2023)—offers a different approach by treating each data point  $x$  as a continuous function without discretization.

*Remark: Opportunities:* The cases of manifold-valued signals on manifold domain, topological-valued signals on topological domains, or topological-valued signals on manifold domains are not included in the table, since they have rarely been considered in the machine learning and deep learning literatures. These classes represents an interesting avenue for future research.

*Remark: Data as Spaces:* Beyond data as coordinates and data as signals, a third class of data types can be considered: *data as spaces*. In this class, a data point may instead represent an entire space: the data point  $x$  is a manifold or topological space itself. For example, consider a dataset of molecules. Each molecule  $x$  can be represented as a distinct graph that captures the molecular structure, with nodes representing atoms and edges representing bonds. The dataset is comprised of the set of different graphs. Alternatively, the dataset may consist of 3D surface scans of the human body, e.g., a dataset of heart surfaces—each data point  $x$  is a distinct manifold. Most of the time, however, there is additional information associated with each data point  $x$ , so that  $x$  is not only a space.

For example, a molecule would not only be described

as the relationships between its atoms, but also as the positions of its atoms, or as the distance between two atoms. In other words, there would be a feature associated to each atom representing the 3D location of the atom. Hence, the molecule would be, in fact, represented as a signal from a graph  $\Omega$  to  $\mathbb{R}^3$ , and not just as a graph: it will fall in the category described by Card S5.

Similarly, processing organ shapes such as heart surfaces requires knowing the 3D coordinates of each point on the surface of the heart. Each heart would be, in fact, represented as a signal from a manifold  $M$  to  $\mathbb{R}^3$  and not just as a manifold. Consequently, these examples fall into the category of data as signals.

In this review, we will use the two main classes of data representations—**as coordinates**, and **as signals**—to characterize non-Euclidean structure in machine learning and deep learning models.

#### IV. SURVEY: NON-EUCLIDEAN MACHINE LEARNING

We now review a large and disparate body of literature of non-Euclidean generalizations of algorithms classically defined for data residing in Euclidean spaces. The generalization of machine learning methods to non-Euclidean data relies on the generalization of their mathematical foundations—probability and statistics—to non-Euclidean spaces. In most cases, this requires non-trivial algorithmic innovations. Such generalizations comprise the bulk of the work reviewed here.

However, we note that there are two “simple” approaches to generalizing Euclidean models that do not require significant algorithmic innovation. They do not work for all algorithms, and they have limitations. Yet, when possible, they have the benefit of implementational simplicity. We briefly describe two classes of such approaches here—what we call “*plug-in*” methods and *tangent space methods*.

### Non-Euclidean Probability and Statistics.

In a non-Euclidean space, many essential mathematical concepts must be modified to respect the inherent structure of the space. Consider, for example, a dataset consisting of points that lie on the surface of the sphere—for example, the coordinates of different cities around the globe. The Euclidean mean of the points is a value that lies off-manifold—a point lying somewhere “inside” the sphere but not on the sphere. To find the centroid of these points on the manifold, we must instead use the **Fréchet mean**, which is defined as the point that minimizes the sum of squared *geodesic distances* to all other points in the dataset. By using geodesics, the Fréchet mean is constrained to the manifold, and results in a natural generalization of the notion of a mean to non-Euclidean space. The field of **Geometric Statistics** defines such non-Euclidean generalizations. We refer the reader to [Pennec \(2006\)](#) for theoretical foundations on manifolds, to [Guigui et al. \(2023\)](#) for a comprehensive introduction to these foundations and to [Pennec et al. \(2019\)](#) for real-world applications.

*“Plug-In” Methods:* The most straightforward way to generalize machine learning methods to non-Euclidean spaces is to simply replace the definitions of addition, subtraction, distances, and means employed in the Euclidean method with their non-Euclidean counterparts. For example, the k-nearest-neighbors algorithm can be naturally defined for arbitrary non-Euclidean manifolds by replacing Euclidean distance with geodesics. Similarly, k-means can be generalized using geodesic distances and the Fréchet mean. Any *kernel method* that makes use of geodesic distance in the kernel function fall into this category as well. Many popular implementations of machine learning algorithms—for example in the `scikit-learn` package—permit the user specification of a distance function, thus facilitating easy generalization to non-Euclidean spaces.

*Tangent Space Methods:* An alternative approach is particularly convenient for non-Euclidean spaces that are manifolds. We call it the tangent space method. It consists in projecting the data from the manifold into the tangent space of a particular point on the manifold, using the so-called *exponential map*. Importantly, the tangent space can be seen as a Euclidean

space. Once the data are mapped to Euclidean space, traditional Euclidean machine learning can be applied. This approach typically achieves better results than applying Euclidean methods directly to the original non-Euclidean data. However, in many cases—particularly for manifolds with greater curvature—it induces biases in the results due to errors in the local Euclidean approximation of the manifold. Nonetheless, the approach is relatively simple, and can be worthwhile for data lying on relatively flat manifolds, or on manifolds that are flat at the scale of the spread of the data.

Both the plug-in and tangent space methods have the advantage of implementational simplicity. However, many machine learning algorithms require more than just the specification of distances and means, which limits the applicability of the plug-in method. Additionally, in many cases, the biases induced by the tangent space projection are intolerable for the application, which limits its scope. Consequently, in many scenarios, it is necessary to explicitly constrain aspects of the algorithms to the manifolds of interest. This comprises the bulk of the work of Non-Euclidean Machine Learning, which we cover in this section. We first cover *regression* methods, followed by *dimensionality reduction* methods. In the following section, we will cover Non-Euclidean Deep Learning methods, which may be used for regression, dimensionality reduction, or classification.

We note that the Non-Euclidean Machine Learning methods reviewed in this paper assume that certain topological, algebraic, or geometric structures are known *a priori* to be present in the data or learning problem. These methods thus require pre-specifying these structures. Sometimes, however, the underlying structure is unknown. A class of methods aims to *discover and characterize unknown non-Euclidean structure* in data. This class includes **topological data analysis**, certain manifold learning approaches that learn parameters of a latent manifold, such as in **metric learning**, and algebraic methods for discovering latent group structure, also known as **group learning**. Such methods can be used to identify the non-Euclidean structures present in data so that the appropriate non-Euclidean machine learning method can be specified and applied. These methods are beyond the scope of this review, as they are used “prior to” non-Euclidean machine learning.

#### A. Regression

This subsection reviews regression on manifolds. We first introduce our taxonomy defined by the mathemati-

cal structure of both the *data spaces* and the regression *model*. Then, we review the literature on this topic in Figure 5 with details in the text.

*Taxonomy:* In machine learning, the problem of regression can be defined as learning a function  $f$  going from an input space  $X$  to an output space  $Y$ . Figure 5 organizes regression models into a taxonomy that is first based on the geometric properties of input and output spaces—see first two columns in Figure 5. Here, we differentiate conventional Euclidean spaces from more complex manifold spaces, setting the stage for a detailed exploration of five key configurations: Euclidean to Euclidean, one-dimensional Euclidean to Manifold, Euclidean to Manifold, Manifold to Euclidean, and Manifold to Manifold.

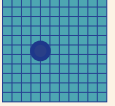
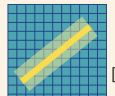
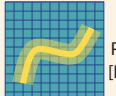
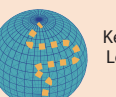
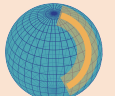
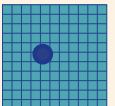
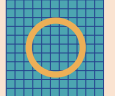
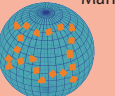
Each configuration is then distinguished by its regression model—see third column in Figure 5. *Linear* methods assume a relationship between the input variable  $x \in X$  and output variable  $y \in Y$  that can be represented by a linear function as  $y = \mathbf{A}x + \mathbf{b}$ , where  $\mathbf{A}$  is a matrix of coefficients, and  $\mathbf{b}$  is a vector of constants—hence constraining the  $y$ 's to belong to a linear space characterized by the parameters  $A, b$ . We note that linear regressions are not appropriate on manifolds since the addition operation, a linear operation, is not well-defined on a manifold, a non-linear space. Consequently, linear methods become *geodesic* methods on manifolds on rows 2 and 3 of Figure 5, where the relationship between  $x$  and  $y$  can be represented by a geodesic characterized by a set of parameters analogous to  $A, b$  above. Next, *non-linear parametric* and *non-geodesic parametric* methods involve relationships described by a fixed set of parameters but in a more complex form, such as polynomials or other non-linear equations  $y = f_{\theta}(x)$  where  $\theta$  represents the parameters. *Non-parametric* approaches, on the other hand, do not assume a parametric form for the relationship between  $x$  and  $y$ , providing flexibility to model relationships that are directly derived from data. The term nonparametric does not necessarily mean that such models completely lack parameters but that the number and nature of the parameters are flexible and not fixed in advance, contrarily to parametric approaches.

Further, these methods are categorized as *Bayesian* or *non-Bayesian*—represented by a fuzzy line or a line in Figure 5. *Bayesian* methods integrate prior probabilistic distributions with observed data, facilitating the updating of knowledge about the parameters in light of new evidence. This approach contrasts with *non-Bayesian* methods, which rely exclusively on observed

data, typically employing so-called frequentist statistical principles without incorporating prior distributions on parameters.

In what follows, we review regression models according to this geometric taxonomy, row by row in Figure 5. For each category of regression models, we showcase one emblematic, category-defining, paper that reflects the transition from traditional Euclidean analysis to the manifold paradigm. We consider the following papers to be *out of scope*: 1) Papers that generalize a class of curves (e.g., splines) on manifolds, but do not leverage this generalization to perform regression, 2) Papers that perform interpolation on manifolds, but not regression, 3) Papers whose regression method has been developed for only one type of manifold (e.g., only for spheres). Additionally, the methods reviewed in this section exclusively apply to one of the data types presented in Section III: regression inputs  $x$  and outputs  $y$  are data as coordinates in a space, where the space is either a Euclidean space or a manifold.

- 1) **Euclidean Input, Euclidean Output:** We review classical regression models that have been generalized to manifolds, in the first row of Figure 5. Initiated with linear regression by Legendre and Gauss (Legendre, 1805), this category has expanded to include nonlinear parametric models, particularly polynomial models introduced by Gergonne (Gergonne, 1815). The inclusion of non-parametric methods is marked by the Nadaraya-Watson kernel methods (Nadaraya, 1964), further local linear models (Fan, 1993), and Breiman's development of random forests (Breiman, 2001). In Bayesian analysis, the linear and polynomial approaches are respectively represented by Bayesian Multilinear (Box and Tiao, 1968) and Polynomial Bayesian models (Halpern, 1973), with the Gaussian Process (Williams and Rasmussen, 1995) illustrating the non-parametric Bayesian perspective.
- 2) **One-dimensional Euclidean Input, Manifold Output:** The earlier generalizations of classical regression models to manifolds involve generalizing the output space. Many of these models consider a one-dimensional input  $x$ , and are shown in the second row of Figure 5. Geodesic regression extends linear models into manifolds from one-dimensional Euclidean inputs (Fletcher, 2011). We note a difference of 206 years between the establishment of linear regression to its geometric counterpart. Polynomial regressions on manifolds

Geometric Structures in Regression					
Regression Input	Regression Output	Regression Model			
		Linear 	Parametric 	Nonparametric 	
$x \in \mathbb{R}^m$ 	$y \in \mathbb{R}^{m'}$ 	Non Bayesian	 Multilinear [Pearson1898]	 Polynomial [Gergonne1815] Bézier [Casteljau1985]	 Kernel [Nadaray-Watson64] Local Linear [Fan93] Random Forests [Breiman01]
		Bayesian	 Bayesian Multilinear [Box, Tiao 68]	 Bayesian Polynomial [Halpern73]	 Gaussian Process [Rasmussen03]
$x \in \mathbb{R}$ One-dim. 	$y \in M'$ 	Non Bayesian	 Geodesic [Fletcher11]	 Manifold Polynomial [Hinkle14] Manifold Bézier Spline [Hanik20]	 Kernel [Davis10] Local Geodesic [Schotz22]
		Bayesian	 Bayesian Geodesic [Zhang20]	 Manifold Bayesian Polynomial [Muralidharan17]	 Brownian [Wang15]
$x \in \mathbb{R}^m$ 	$y \in M'$ 	Non Bayesian	 Fréchet [Petersen17]	 Convolution Regression [Pennec06]	 Manifold Random Forest [Tsagkraloulis18] Local Fréchet [Petersen17] Local Extrinsic [Lin17]
		Bayesian	 Opportunity	 Manifold Gaussian Process [Yang16] Wrapped Gaussian Process [Mallasto18]	
$x \in M$ 	$y \in \mathbb{R}^{m'}$ 	Non Bayesian	 Circular [Chernov10] [Johnson78]	 Manifold Kernel [Pelletier05]	
$x \in M$ 	$y \in M'$ 	Non Bayesian	 Regression after tangent PCA [Guo20]	 Manifold Regular splines [Steinke08] Manifold Kernel [Banerjee15] [Zhang2020]	

**Fig. 5: Geometric Structures in Regression** categorized according to the geometry of the input and output data spaces (first two columns) and the geometry of the regression model (last column). Yellow boxes correspond to Euclidean space, while orange corresponds to non-Euclidean space. Partially Euclidean cases are light orange. Each pictogram represents the kind of parametrization used: linear (geodesic), nonlinear (nongeodesic) parametric, or nonparametric, with or without Bayesian priors.

(Hinkle et al., 2012a) and Bezier-splines fitting on manifolds (Hanik et al., 2020) generalize their Euclidean counterparts to manifolds in the output space, 197 years and 35 years later respectively. Non-parametric methods with output values on manifolds include Fréchet-casted Nadaraya-Watson kernel regression (Davis et al., 2010), and local geodesic regression (Schötz, 2022)—the latter being the counterpart of local linear regression to manifolds. In terms of Bayesian methods, the geodesic regression model was made Bayesian in (Zhang et al., 2020), while manifold polynomial regression turned Bayesian in Muralidharan et al. (2017). Lastly, one non-geodesic, non-parametric, Bayesian model belongs to this category: kernel regressions by Devito and Wang’s Brownian motion model (Wang, 2015) which generalizes Nadaraya-Watson’s approach 51 years later.

- 3) **Euclidean Input, Manifold Output:** Next, we review regression models with outputs on a manifold, for which the input is not restricted to be one-dimensional, in the third row of Figure 5. The Fréchet regression (Petersen and Muller, 2016) generalizes the geodesic regression to higher-dimensional Euclidean inputs. We also find several nongeodesic parametric regression models. One of the earliest works in this category deals with the parametric regression of regularized manifold valued functions (Pennec et al., 2006). A key idea is to rephrase convolutions as weighted Fréchet means of manifold variables, which become the parameters of the implicit function. Also in the nongeodesic parametric regression category, we find the semi-parametric intrinsic regression model by (Shi et al., 2009), or the stochastic development regression by Kühnel and Sommer (2017). Non-parametric methods with manifold-valued outputs include the manifold random forests (Tsagkrasoulis and Montana, 2018) that generalize their Euclidean counterpart 15 years later, the local Fréchet regression (Petersen and Muller, 2016), another multi-dimensional generalization of the local linear regression, and the local extrinsic regression by (Lin et al., 2017). In terms of Bayesian approaches, we observe a lack of methods within geodesic and nongeodesic parametric models. However, we find Bayesian non-parametric methods, such as Manifold Gaussian processes (Yang and Dunson, 2016) and Mallasto’s wrapped Gaussian processes (Mallasto and Feragen, 2018) which generalizes Williams and Rasmussen’s Gaussian processes 9 and 13

years later.

- 4) **Manifold Input, Euclidean Output:** We now review geometric generalizations of Euclidean regression models that have received less attention: models in which the regression input space is a manifold. We start with methods for which the output space is a Euclidean space, in the fourth row of Figure 5. Johnson and Wehrly defined a regression model for an angular (one-dimensional) variable with a Euclidean scalar (one-dimensional) output variable (Johnson and Wehrly, 1978). Chernov’s circular regression outputs to higher-dimensional Euclidean spaces, typically two- or three-dimensional (Chernov, 2010). Pelletier’s non-parametric regression approach stands out for estimating functions from manifold inputs to Euclidean outputs (Pelletier, 2006). Both methods are non-Bayesian. In terms of Bayesian methods, we find the Bayesian circular-linear regression method (Gill and Hangartner, 2010), but no Bayesian nonparametric methods—indicating an opportunity for further exploration.
- 5) **Manifold Input, Manifold Output:** The fifth row of Figure 5 presents the most general case of regression, from a geometric perspective. In these models, both the regression input and output spaces are manifolds. This category includes a method that first transforms both input and output data from manifolds to Euclidean spaces, and then apply an auxiliary classical regression model on Euclidean spaces (Guo et al., 2019). In the nonparametric methods, we find Steinke’s regular splines methods (Steinke et al., 2008) and Banerjee’s manifold kernel regression (Banerjee et al., 2015) generalizing in 2015 both the classical kernel regression from 1964 and its generalization to manifold output space from 2010. At the time of the review, there is no method in this category that adopts the Bayesian point of view.

## B. Dimensionality Reduction

This subsection reviews dimensionality reduction methods, which include: manifold learning methods, where a manifold of lower-dimension is learned within a Euclidean space of higher dimension; submanifold learning methods, where a submanifold of lower-dimension is learned within a manifold of higher dimension; and encoding methods, where data in a high-dimension Euclidean or manifold is mapped to a lower-dimensional Euclidean or manifold via an encoder. We first introduce our taxonomy defined by

the mathematical structure of both the *spaces* and the dimensionality reduction *model*. Then, we review the literature on this topic in Figure 6 with details in the text.

*Taxonomy*: We define the problem of dimensionality reduction as transforming high-dimensional data from their data space  $X$  into a latent space  $Y$  of lower dimension, i.e.,  $\dim(Y) < \dim(X)$ . Figure 6 organizes dimensionality reduction methods into a taxonomy first based on the geometric properties of the data and latent spaces—see the first two columns. It differentiates between conventional Euclidean spaces and the more complex manifold spaces, setting the stage for the following four key configurations: Euclidean Data to Euclidean Latents, Manifold Data to One-Dimensional Euclidean Latents, Manifold Data to Euclidean Latents, Euclidean Data to Manifold Latents, and Manifold Data to Manifold Latents. For each configuration, the lower dimensional latent space  $Y$  is schematically represented as a space of dimension 1: a line for Euclidean spaces, and a circle for manifolds. The higher-dimensional data space  $X$  is schematically represented as a space of dimension 2: a plane for Euclidean spaces, and a sphere for manifolds. Yet, we emphasize that we review all dimensionality reduction methods here; not only the methods going from dimension 2 to dimension 1.

Each configuration is then distinguished by the approach to dimensionality reduction—see third column in Figure 6. First, dimensionality reduction approaches are organized depending on whether they leverage a decoder, and if so, of what type: linear (resp. geodesic), nonlinear (resp. nongeodesic) parametric, non-parametric—represented by full line, full curved line, and dashed curved line in the pictograms of Figure 6. While every dimensionality reduction method converts high-dimensional data into lower-dimensional latents, only some methods introduce a decoder  $D$  that converts low-dimensional latents  $y$ 's back into high-dimensional data  $x$ 's:  $x = D(y)$ . When a decoder  $D$  exists, the latent space  $Y$  can be embedded into the data space  $X$  via  $D(Y) \subset X$ . The yellow and orange curves in the pictograms represent that embedding. We further distinguish two subcases: whether the embedded space  $D(Y)$  is linear (geodesic, in the manifold case), or nonlinear (or non-geodesic). The presence of a decoder is represented by a black arrow and the legend  $D$ ; the black arrow is a dotted arrow if the decoder is non-parametric. Dimensionality reduction methods that do not leverage any decoder are reviewed independently at the bottom of Figure 6.

Additionally, we highlight in the pictograms if the data is assumed to come from a generative model. A generative model explains how data points are generated from latents using probability distributions. When a generative model is used for a given dimensionality reduction approach, it is denoted by a shaded yellow or orange dot. When there is no generative model, we only use a non-shaded yellow or orange dot. For example, principal component analysis (PCA) has a decoder, but no generative model; while probabilistic PCA uses a decoder with a generative model.

Second, approaches are organized depending on whether they leverage an encoder  $E$ , where  $E$  is a function mapping data  $x$ 's to latents  $y$ 's:  $E(x) = y$ . Indeed, while every dimensionality reduction methods converts high-dimensional data into lower-dimensional latents, only some methods do so through an explicit encoder function  $E$ . Others might only compute the latent  $y_i$  corresponding to a data point  $x_i$  through the result of an optimization  $\min_y \text{Cost}(x_i)$ . The presence of an encoder is represented by a black arrow and the legend  $E$ , and the arrow is a dotted arrow if the encoder is non-parametric. The use of optimization is represented by the ! and no black arrow.

Third, approaches are organized depending on whether they compute an uncertainty on the latents  $y$  associated with the data points  $x$ . Uncertainty on the latents is represented by the posterior distribution  $p(y|x)$ . If the method provides a posterior distribution—or at least an approximation of it—we use a shaded blue dot. If not, we use a non-shaded blue dot. The two cases of without and with posterior form the subrows of a given configuration in the table. We mark with an  $S$  the cases where the posterior distribution  $p(y|x)$  is not computed analytically, but provided through a sampling approach.

Fourth, approaches are categorized based on how they compute uncertainty on the parameters of the decoder, i.e., on whether they are Bayesian or not. For example, traditional PCA does not incorporate uncertainty, but Bayesian PCA does. This distinction represents the last subrow of each configuration, illustrated by a shaded orange line.

We now survey the various categories of dimensionality reduction row by row in Figure 6.

- 1) **Euclidean Data, Euclidean Latents**: We describe approaches from this configuration subcolumn by subcolumn. Principal Component Analysis (PCA) (Pearson, 1901) learns a linear subspace, while Probabilistic PCA (PPCA) (Tipping

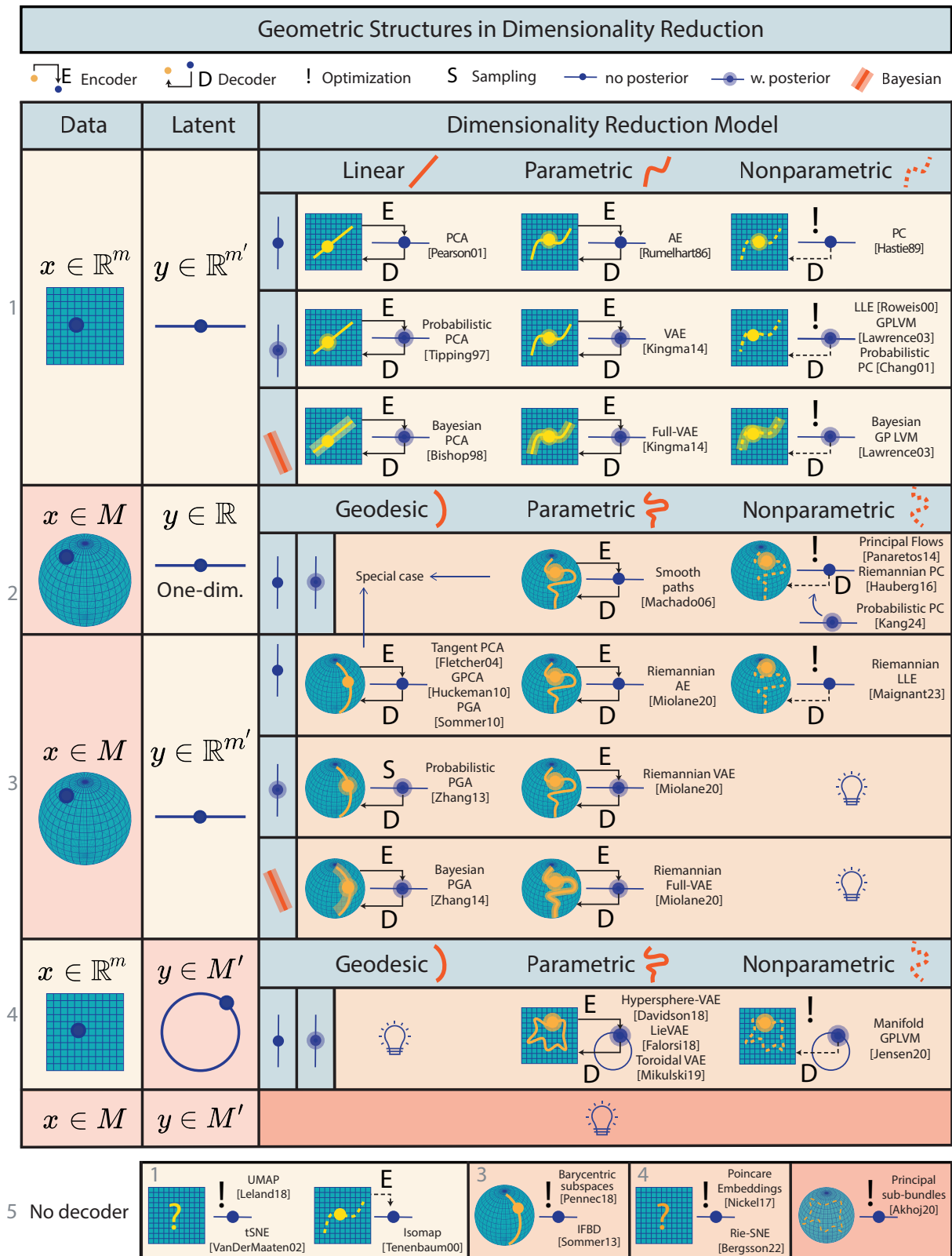


**Fig. 6: Geometric Structures in Dimensionality Reduction** categorized according to the geometry of the data and latent spaces (first two columns) and of the dimensionality reduction model (last column). Yellow boxes correspond to Euclidean space, while orange corresponds to non-Euclidean space. Partially Euclidean cases are light orange. Each model is further classified by use and type of encoder/decoder, as well as whether it computes a posterior on the latents, and whether it is Bayesian. (P)PC: (Probabilistic) Principal Curves; GP LVM: Gaussian Process Latent Variable Model; PGA: Principal Geodesic Analysis; GPCA: Geodesic PCA.

and Bishop, 1999) achieves the same goal within a probabilistic framework relying on a latent variable generative model, which provides a posterior distribution on the latents. Bayesian PCA (Bishop, 1998) additionally learns a probability distribution on the parameters of the models, representing the parameters of the linear subspace (e.g., slope and intercept). These methods are restricted in the type of subspace that can be fitted to the data: only linear subspaces. To lift this restriction, we also find numerous methods that learn nonlinear manifolds from Euclidean data. The whole field of manifold learning fits in this case, and can be subdivided into further subcategories depending on *how* the learned manifold is being represented: by a nonlinear parametric decoder, by a nonparametric decoder, or without any decoder at all. Here, we only introduce one category-defining method for each of the subcategories we consider.

In the nonlinear parametric decoder category, we introduce autoencoders. Autoencoders (AEs) (Rumelhart et al., 1986) learn a nonlinear subspace of a Euclidean space, while variational autoencoders (VAES) (Kingma and Welling, 2014) achieve the same goal with a probabilistic framework relying on a latent variable generative model. The Full-VAE model proposed in (Kingma and Welling, 2014) additionally learns a posterior on the parameters of the model, i.e., the parameters of the decoder. The methods in these category all leverage an encoder. In the nonparametric decoder category, we introduce principal curves (Hastie and Stuetzle, 1989), which fit a nonlinear manifold to the data, but do not leverage a posterior on the latents. In this same category, we also introduce Local Linear Embedding (LLE) (Roweis and Saul, 2000) and Gaussian Process Latent Variable Models (GP LVM) (Lawrence, 2003), which all provide posteriors on the latents. A probabilistic approach to principal curves (PPS) developed in Chang and Ghosh (2001) also falls under this category. Finally, we introduce the Bayesian GP LVM, which additionally provides a posterior on the model’s parameters. We note that the methods of this category do not leverage any encoder, and instead compute the latent associated to a given data point by solving an optimization problem.

These techniques are based on vector space operations that make them unsuitable for data on manifolds. As a consequence, researchers have

developed methods for manifold data, which take into account the geometric structure; see next row in the Table, described in the next paragraph.

- 2) **Manifold Data, One-Dimensional Euclidean Latents:** Fitting a geodesic to manifold data points has been performed using least-squares or other likelihood criteria in many domains, in particular as a first step of the extension of PCA to manifolds (see next paragraph). In the nongeodesic parametric decoder category, a natural extension with one-dimensional latents is to define approximating splines using higher order polynomials that are then fitted to a set of points on a Riemannian manifold (Machado et al., 2010, Machado and Leite, 2006) or on a Lie group (Gay-Balmaz et al., 2012). In the nongeodesic, nonparametric decoder category, principal flows (Panaretos et al., 2014) and Riemannian principal curves (Hauberg, 2016) generalize traditional Euclidean principal curves to Riemannian manifolds, 25 years later. The probabilistic Riemannian principal curves (Kang and Oh, 2024) further introduce a probabilistic framework relying on a latent variable generative model, hence generalizing the Euclidean probabilistic principal curves, 23 years later.
- 3) **Manifold Data, Euclidean Latents:** We describe approaches subcolumn by subcolumn. We note that approaches from this configuration can be applied to the previous configuration, i.e., to one-dimensional latent spaces as well. In the geodesic decoder category, Principal Geodesic Analysis (PGA) (Fletcher et al., 2004, Sommer et al., 2014), tangent PGA (tPGA) (Fletcher et al., 2004), and Geodesic Principal Component Analysis (GPCA) (Huckemann et al., 2010). learn variants of geodesic subspaces, generalizing the concept of a linear subspace to manifolds. As such, these methods represent different generalizations of PCA to manifolds. Probabilistic PGA (Zhang and Fletcher, 2013) achieves the same goal, while adding a latent variable model generating data on a manifold, and hence generalizes probabilistic PCA, 16 years later. Similarly, Bayesian PGA (Zhang and Fletcher, 2013) generalizes Bayesian PCA by including the posterior distribution of the parameters defining the submanifolds, i.e., the base point and tangent vectors defining the principal (geodesic) components. However, these methods are restricted in the type of submanifold that can be fitted to the data, that is: geodesic

subspaces at a point.

The restriction to globally defined subspaces based on geodesics can be considered both a strength and a weakness. While it protects from the problem of overfitting with a submanifold that is too flexible, it also prevents the method from capturing possibly nonlinear effects. With current dataset sizes exploding (even within biomedical imaging datasets which have been historically much smaller), the investigation of flexible submanifold learning techniques may become increasingly important.

In the nongeodesic parametric decoder category, we consider autoencoder approaches on manifolds. Variational autoencoders have been generalized to manifold data in (Miolane and Holmes, 2020), a methodology that can be applied to both AEs and Full-VAEs on manifolds. This is the only method that learns a multidimensional nongeodesic submanifold parameterized with a latent variable model. Lastly, we feature a method that leverages a nonparametric decoder: the Riemannian LLE (Maignant et al., 2023), which generalizes its Euclidean counterpart, the LLE, 23 years later. We note the absence of works performing dimensionality reduction via a nonparametric decoder in a generative model nor in a Bayesian framework. This represents a possible avenue for research.

- 4) **Euclidean Data, Manifold Latents.** We describe approaches from this configuration subcolumn by subcolumn. We first find approaches that belong to the VAE framework, where the latent space is a manifold, even though the data belong to a Euclidean space. For example, the hypersphere VAE by Davidson et al. (2018) proposes a hyperspherical latent space, Falorsi et al. (2018) propose a Lie group latent space, and Mikulski and Duda (2019) propose a toroidal latent space. All of these approaches provide an (approximate, amortized) posterior on the latent variables, represented as a probability distribution on the manifold of interest. In some sense, these approaches represent the counterpart of Miolane and Holmes (2020) which considers a manifold data space and a Euclidean latent space. Next, we find nonparametric decoder approaches, such as the manifold Gaussian Process Latent Variable Model (GPLVM) (Jensen et al., 2020) which generalizes the GPLVM from the Euclidean case (Lawrence, 2003).

- 5) **No Decoder.** Few dimensionality reduction models avoid using a decoder. For this reason, we briefly survey these models across all geometric data and latent structures. In the Euclidean data with Euclidean latent case (corresponding to row 1), we find t-distributed stochastic neighbor embedding (tSNE) (van der Maaten and Hinton, 2008), Uniform Manifold Approximation and Projection (UMAP) (McInnes et al., 2018) and Isomap (Tenenbaum et al., 2000). These approaches learn lower-dimensional representations of data but do not provide a latent variable generative model, nor a parameterization of the recovered subspace. In the manifold data with Euclidean latent case (corresponding to row 3), a flexible generalization of linear subspaces to manifolds is given by barycentric subspaces (Pennec, 2018) where the submanifold is defined implicitly through geodesics to several reference points. One approach of interest in this line of work is to provide *sequences* of nested spaces of increasing dimensions that better and better approximate the data, a notion conceptualized by (Damon and Marron, 2013) with sequences of nested relations of possibly non-geodesic subspaces. Iterated Frame Bundle Development (IFBD) (Sommer, 2013) is another optimization method iteratively building principal coordinates along new directions. In the Euclidean data with manifold latent case (corresponding to row 4), we first find the Poincaré embeddings Nickel and Kiela (2017) that embeds data points in  $X$  into a hyperbolic latent space  $Y$ , which is useful for representing data with hierarchical structure. We note that this approach does not leverage any encoder function  $E$ , and instead solves an optimization problem to find the latent variable  $y_i$  that corresponds to each data point  $x_i$ , represented on the Figure 6 by the pictogram “!”. Second, the Riemannian SNE (Bergsson and Hauberg, 2022) generalizes traditional Euclidean SNE (van der Maaten and Hinton, 2008) but 14 years later. Finally, the last decoder-free model, called principal subbundles (Akhøj et al., 2023), is the only dimensionality reduction model designed for manifold data and manifold latents. Indeed, we note that there are no decoder-based approaches for dimensionality reduction for this case. The principal subbundles method does not leverage either an encoder or decoder, but instead solves optimization problems to find the low-dimensional latent variable  $y_i$  associated with each data point  $x_i$ . The authors also

propose a decoding approach that uses optimization rather than an explicit decoder to find the data point  $x_i$  that decodes a given latent variable  $y_i$ . Overall, the sparsity of decoder-free dimensionality reduction models leaves open opportunities for many choices of geometric data/latents.

This concludes our review and categorization of non-Euclidean generalizations of machine learning methods for regression and dimensionality reduction. While several deep neural network models—such as variational autoencoders—appear in our dimensionality reduction taxonomy, we have saved a more complete treatment of deep learning for the next section. Deep neural networks stand out from more traditional machine learning methods in that they are flexible compositions of functions that progressively transform data between spaces. In our consideration of dimensionality reduction methods, we abstracted away from the transformations performed by individual neural network layers to consider only the structure of the input and latent spaces (which may be many layers deep in a model). In the next section, we explicitly consider the input-output structure of individual neural network layers, and the ways in which topology, geometry, and algebra have been incorporated into these layers.

## V. SURVEY: NON-EUCLIDEAN DEEP LEARNING

We now review non-Euclidean structures in deep learning, particularly focusing on how geometry, topology, and algebra can enrich the structure of a given layer within a deep neural network. A neural network layer is a function  $f : X \rightarrow Y$ , and thus can be analyzed and categorized in terms of the mathematical structure of the input space  $X$  and output space  $Y$ . We first cover neural network layers without an attention mechanism, followed by layers with attention. We then compile a list of datasets and benchmarks used in the literature to compare deep learning methods with geometric, topological, or algebraic properties.

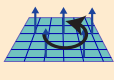
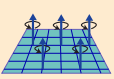
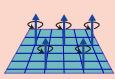
### A. Neural Network Layers Without Attention

We categorize *layers* from neural networks according to their mathematical structure. A given paper can appear several times in this subsection (and the next), if this paper introduces several novel layers. Neural networks using the attention mechanism are out of scope for this subsection and will be presented in the next subsection.

*Taxonomy:* Figure 7 organizes deep learning methods into a taxonomy based on the mathematical properties of the input and output of neural network layers (first two columns), as well as on the properties of the layer model (third column). The rows show different types of layers that have been published in the literature, organizing them by use of geometry, algebra (group actions), and topology. The figure graphically contextualizes existing methods and identifies potential areas for innovation. We survey the field row by row in Figure 7.

*Geometry in Neural Network Layers:* Here, we categorize neural network layers that consider their inputs and outputs as coordinates in space, where the spaces can be equipped with geometric structures.

- 1) **Euclidean input, Euclidean output:** The category-defining layer for this configuration is the Perceptron layer (Rosenblatt, 1958), commonly used as a component in a deep neural network comprised of several identical layers: the celebrated Multi-Layer Perceptron (MLP).
- 2) **Euclidean input, manifold output:** The Perceptron-Exp layer from Miolane and Holmes (2020) generalizes the Perceptron layer to layer outputs on manifolds. Here, Exp denotes the Riemannian exponential map, which is applied to the result of the Perceptron. Indeed, Exp is an operation that maps tangent vectors to points on a manifold, i.e., that maps an input in an Euclidean space to an output on the manifold. Only the Perceptron component of this layer has learnable weights; the manifold needs to be known a priori in order to specify and implement the appropriate exponential map. Additionally, in general, there is no analytical expression for the Exp map, which needs to be computed numerically. To avoid this computational cost, this layer is best implemented for manifolds whose Exp enjoys an analytical expression.
- 3) **Manifold input, Euclidean output:** The Log-Perceptron layer from (Davidson et al., 2018) generalizes the Perceptron layer to layer inputs on manifolds. Here, Log denotes the Riemannian logarithm map, which is applied just before the Perceptron. Indeed, Log is an operation that maps points on manifolds to tangent vectors; that is, it is the inverse of the Exp. The layer maps an input on a manifold to an output in Euclidean space where the Perceptron with its learnable weights can be applied. This layer can thus be thought of as the inverse of the Perceptron-Exp layer from Miolane

Topology, Geometry, and Algebra in Neural Network Layers					
Layer Input	Layer Output	Layer Model	Layer Input	Layer Output	Layer Model
$x \in \mathbb{R}^n$ 	$y \in \mathbb{R}^{n'}$ 	 Perceptron	$x : M \rightarrow \mathbb{R}^n$ 	$y : M \rightarrow \mathbb{R}^{n'}$ 	Regular Gauge-Convolution [Cohen19a]
$x \in \mathbb{R}^n$ 	$y \in M$ 	 Perceptron-Exp from Riemannian VAE [Miolane20]	$x : M \rightarrow \mathbb{R}^n$ 	$y : M \rightarrow \mathbb{R}^{n'}$ 	Gauge-Convolution with induced representation [Cohen19a]
$x \in M$ 	$y \in \mathbb{R}^{n'}$ 	 Log-Perceptron from Hypersphere VAE [Davidson18]	$x : P \rightarrow \mathbb{R}^n$ 	$y : P \rightarrow \mathbb{R}^{n'}$ 	PointNet++ [Qi17]
$x \in M$ 	$y \in M$ 	 BiMap layer from [Huang16] ManifoldNet layer from [Chakraborty22]	$x : P \rightarrow \mathbb{R}^n$ 	$y : P \rightarrow \mathbb{R}^{n'}$ 	Tensor Field Networks [Thomas18] PONITA [Bekkers24]
$x \in \mathbb{R}^n$ 	$y \in \mathbb{R}^{n'}$ 	 Equivariant-Perceptron from [Finzi21] Linear layer from GATr [Brehmer23]	$x : G \mapsto \mathbb{R}^n$ 	$y : G \mapsto \mathbb{R}^{n'}$ 	Graph convolution [Kipf17] Message passing [Gilmer17]
$x : \mathbb{R}^n \rightarrow \mathbb{R}^{n'}$ 	$y : \mathbb{R}^m \rightarrow \mathbb{R}^{m'}$ 	Convolutional [Lecun] Regular Steerable Euclidean [Cohen17]	$x : G \mapsto \mathbb{R}^n$ 	$y : G \mapsto \mathbb{R}^{n'}$ 	E(n)-EGNN [Satorras2021]
$x : \mathbb{R}^n \rightarrow \mathbb{R}^n$ 	$y : \mathbb{R}^{n'} \rightarrow \mathbb{R}^{n'}$ 	Steerable Convolutional [Cohen17]	$x : \Omega \mapsto \mathbb{R}^n$ 	$y : \Omega \mapsto \mathbb{R}^{n'}$ 	Simplicial and cellular convolution [Ebl120, Roddenberry22] Simplicial and cellular message-passing [Bodnar21, Hajji20]
$x : \mathbb{R}^n \rightarrow \mathbb{R}^n$ 	$y : G_p \rightarrow \mathbb{R}^{n'}$ 	Regular Group-Convolution (first layer) [Cohen16]	$x : \Omega \mapsto \mathbb{R}^n$ 	$y : \Omega \mapsto \mathbb{R}^{n'}$ 	E(n)-EMPSN [Eijkelboom2023] Clifford-EMPSN [Liu2024]
$x : G_p \rightarrow \mathbb{R}^n$ 	$y : G_p \rightarrow \mathbb{R}^{n'}$ 	Regular Group Convolution (second layer) [Cohen16]	$x : \Omega \mapsto \mathbb{R}^n$ 	$y : \Omega \mapsto \mathbb{R}^{n'}$ 	Hypergraph convolution [Arya20] Message passing [Heydari22]
$x : G_p/H \rightarrow \mathbb{R}^n$ 	$y : G_p/H \rightarrow \mathbb{R}^{n'}$ 	General Steerable with quotient representation [Cohen17]	$x : \Omega \mapsto \mathbb{R}^n$ 	$y : \Omega \mapsto \mathbb{R}^{n'}$ 	Combinatorial convolution [Hajji22] Message passing [Hajji22]
$x : G_p/H \rightarrow \mathbb{R}^n$ 	$y : G_p/H \rightarrow \mathbb{R}^{n'}$ 	Group Convolution on homogeneous spaces [Cohen19b]	$x : \Omega \mapsto \mathbb{R}^n$ 	$y : \Omega \mapsto \mathbb{R}^{n'}$ 	E(n)-Equivariant TNN [Battiloro24]

**Fig. 7: Topology, Geometry, and Algebra in Neural Network Layers** organized according to the mathematical properties of the layer inputs  $x$  and outputs  $y$  (first two columns) and of the layer model (third column). The first five rows show inputs and outputs that are data represented as coordinates in a space, typically, a Euclidean space  $\mathbb{R}^n$  or a manifold  $M$ . The next rows show inputs and outputs that are signals, i.e., functions from a domain to a codomain. The black curved arrows represent a group action on a space, such as a signal's domain or codomain. Notations:  $\mathbb{R}^n$ : Euclidean space;  $M$ : Manifold;  $G_p$ : group,  $G_p/H$  Homogeneous manifold for the group  $G_p$ ;  $P$ : point set;  $G$ : graph;  $\Omega$ : topological space.

and Holmes (2020). Just as for the Perceptron-Exp, the manifold needs to be known for this layer to be implemented, and manifolds whose Log enjoys an analytical expression are preferred.

- 4) **Manifold input, manifold output:** This configuration is first illustrated with the Bimap and SPDNet layers from (Huang and Van Gool, 2016), where SPD refer to symmetric positive definite matrices. This layer is indeed restricted to the manifolds of SPD matrices. More generally, ManifoldNet (Chakraborty et al., 2022) builds on the reformulation of convolutions as weighted Fréchet means of Pennec et al. (2006) to propose a layer whose inputs and outputs are both coordinates on a manifold. In this layer, a weighted mean of the inputs is computed, where the weights are learned with classical back propagation. Since convolutions are equivalent to computing weighted sums, this layer has also been termed the manifold-valued data convolution. We note that, in general, there is no analytical expression for the weighted Fréchet mean, which needs to be obtained by optimization. To avoid this computational cost, approximations using tangent means are also considered.

*Algebra in Neural Network Layers:* Here, we consider neural network layers that fall into the category of *equivariant deep learning*, which leverages the concepts of symmetries and group actions. We refer the reader to Cohen et al. (2021) and Weiler et al. (2024) for extensive treatments of the foundations of this field. A core idea underlying this line of work is to build the symmetries natural to a data domain (e.g. translational and rotational symmetries for object classification) into the structure of the model. This facilitates weight sharing across different transformations so that the same convolutional filter can be used to detect a given feature in an image in, for example, all orientations. To accomplish this, the input and output spaces of these layers are equipped with group actions, and the equations defining the layer are written to be compatible with these actions. Intuitively, if a layer is *equivariant* to a group action, this means that, if the layer produces an output  $y$  for a given input  $x$ , then it should also produce a transformed  $y$  for any transformed  $x$ —where transformed here means “acted upon by the same group element.” Here, we highlight key examples of different equivariant layers that fall into each category of our taxonomy.

- 5) **Input and output: Euclidean with group action.** The Equivariant-Perceptron layer from (Finzi

et al., 2021) and the linear layer in the Geometric Algebra Transformer (GATr) (Brehmer et al., 2023) illustrate this configuration. They represent the only equivariant layers processing inputs and outputs that are coordinates in space, as opposed to signals over a space. The work by (Finzi et al., 2021) allows us to build an Equivariant-Perceptron layer given any matrix group action on the input and output spaces.

- 6) **Input and output: Euclidean signal on Euclidean domain with group action.** While the previous row focused on data as coordinates in space, this row considers data as signals. Indeed, both inputs and outputs are defined by function  $x : \mathbb{R}^n \mapsto \mathbb{R}^{n'}$  and  $y : \mathbb{R}^m \mapsto \mathbb{R}^{m'}$ . For example, the input and output could be images, or feature maps, defined over the domains  $\mathbb{R}^n$  and  $\mathbb{R}^m$  respectively. The classic convolutional layer (LeCun et al., 1998) is a layer with translation equivariance: a translation of the input image  $x$  yields a translated feature map  $y$  as output. Regular steerable convolutional layers (Cohen and Welling, 2017) generalize this approach to more complicated cases of equivariances, using groups beyond the group of translations. In this row, the group action is only on the domain of the input and output signals: this is the meaning of the adjective “regular” in regular steerable convolutions.
- 7) **Input and output: Euclidean signal with group action on Euclidean domain with group action.** Similar to the previous row, both inputs and outputs are signals over a space:  $x, y : \mathbb{R}^n \mapsto \mathbb{R}^{n'}$ . By contrast to the previous row, however, both the domain and the codomain of each signal are equipped with a group action. The Steerable Convolutional layer (Cohen and Welling, 2017) illustrates this configuration. Compared to the other layer from the same paper presented above, the group action can affect the domain and codomain simultaneously.
- 8) **Input: Euclidean signal on Euclidean domain with group action; output: Euclidean signal on manifold with group action.** This row presents layers whose input can be described as a signal  $x : \mathbb{R}^n \mapsto \mathbb{R}^{n'}$ , typically an image, and whose output is a more complicated signal of the form  $y : G_p \mapsto \mathbb{R}^{n'}$ , i.e., defined over a Lie group  $G_p$ —where we recall that a Lie group is a manifold that is also a group. The first layer of the Group Convolutional Network by (Cohen and Welling, 2016) illustrates this configuration.

In this network, the second layer necessarily inputs the output of the first layer, i.e., inputs a signal defined over a Lie group. Consequently, the second (and following) layers of this neural network are presented in the next row.

- 9) **Input and output: Euclidean signal on manifold with group action.** Here the manifold domains of both the input and output signals are equipped with a group action. The second layer of the Group Convolutional Network by (Cohen and Welling, 2016) showcases this example, where the manifold is in fact a Lie group, and the group action is the group composition.
- 10) **Input and output: Euclidean signal on homogeneous manifold with group action.** This row presents layers processing inputs and outputs represented as signals of the form  $x, y : G_p/H \mapsto \mathbb{R}^n$ . Here, the domain  $G_p/H$  defines a so-called homogeneous manifold, that is: a manifold equipped with a group action that is such that, for every pair of points on the manifold, there exists a group element that can transform one point onto the other via the action. The General Steerable Convolutional Layer with the so-called quotient representation (Cohen and Welling, 2017) falls in this category.
- 11) **Input and output: Euclidean signal with group action on homogeneous manifold with group action.** Similar to the previous row, signals are represented by functions  $x, y : G_p/H \mapsto \mathbb{R}^n$ , i.e., with an homogeneous manifold domain with group action. By contrast to the previous row, however, there is also a group action on the Euclidean codomains of both the input and the output signals. The group convolutional layer for homogeneous spaces by (Cohen et al., 2019b) falls into this category, as well as the General Steerable layer.
- 12) **Input and output: Euclidean signal on manifold.** In this row, the input and output signals have manifold domains, and Euclidean codomains. Signals are thus represented as  $x, y : M \mapsto \mathbb{R}^n$ . The channel-wise gauge convolutional layer by (Cohen et al., 2019a) processes this type of signals. Here, the concept of gauge equivariance replaces the group equivariance. Gauge equivariance describes the idea of being agnostic to the orientation of a local coordinate systems on the manifold of interest  $M$ .
- 13) **Input and output: Euclidean signal with group**

**action on manifold.** This row generalizes the previous row, where an action can transform elements of the codomains of the signals  $x, y : M \mapsto \mathbb{R}^n$ . An example of this category is the general gauge convolutional layer with induced representation (Cohen et al., 2019a).

*Topology in Neural Network Layers:* Here, we categorize neural network layers that consider their inputs and outputs as signals over a topological domain. We refer the reader to the survey by Papillon et al. (2023) for a comprehensive overview of the neural network layers within this category, and we focus only on selected illustrative examples. These layers are all equivariant to the permutation of the elements of their topological domains: permutation of the points in a set, of the nodes in a graph, etc. As such, all these layers are, at a minimum, equipped with group action on their domain.

- 14) **Input and output: Euclidean signal on a set, with domain group action.** Layers in PointNet++ (Qi et al., 2017) process point clouds, which have signal of the form  $x, y : P \mapsto \mathbb{R}^n$  where  $P$  is a set. In this work, the codomain is restricted to the 2D or 3D Euclidean spaces  $\mathbb{R}^2, \mathbb{R}^3$  as it is designed to process point clouds in 2D or 3D. Thanks to its domain group action, the model is equivariant to a permutation in  $P$ . However, PointNet++ is only approximately invariant to 3D rotations and translations operating in the codomain  $\mathbb{R}^3$ . Namely, it leverages a preprocessing step that first aligns point clouds in position and orientation.
- 15) **Input and output: Euclidean signal on a set, with domain and codomain group actions.** Here, the input and output signals are point clouds, just like the row above. Layers in Tensor Field Networks (TFN) (Thomas et al., 2018), and PONITA (Bekkers et al., 2024) process signals in this category. Like PointNet++, TFN and PONITA process 2D and 3D point clouds and are equivariant to the permutation of their points in  $P$ . TFN and PONITA are additionally equivariant to 3D rotations and translations in  $\mathbb{R}^3$ .
- 16) **Input and output: Euclidean signal on graph, with domain group action.** Layers in this row process signals of the form  $x, y : G \mapsto \mathbb{R}^n$ , i.e., defined over a graph  $G$ . This category is exemplified by Graph Convolutional layer (Kipf and Welling, 2017) and Message Passing layers (Gilmer et al., 2017).
- 17) **Input and output: Euclidean signal on graph,**

- with domain and codomain group action.** Layers in this row are similar to layers in the previous row, except that they add a group action on the codomain of the signals. We find, for example, the  $E(n)$ -Equivariant Graph Neural Networks (EGNN) by (Satorras et al., 2021).
- 18) **Input and output: Euclidean signal on cellular complex, with domain group action.** This row considers signals defined over a cellular complex  $\Omega$ , i.e., functions of the form  $x, y : \Omega \mapsto \mathbb{R}^n$ . Examples include simplicial convolutional (Ebli et al., 2020), cellular convolutional (Roddenberry et al., 2022), simplicial message passing (Bodnar et al., 2021), and cellular message passing (Hajj et al., 2020) layers.
  - 19) **Input and output: Euclidean signal on cellular complex, with domain and codomain group actions.** Layers in this row are similar to layers in the previous row, except that they add a group action on the codomain of the signals. We find, for example, the  $E(n)$ -Equivariant Message Passing Simplicial Networks (EMPSN) (Eijkelboom et al., 2023) and the Clifford group Equivariant Message Passing Simplicial Networks (EMPSN) (Liu et al., 2024) which both introduce group actions on the codomain, but for different groups.
  - 20) **Input and output: Euclidean signal on hypergraph, with domain group action.** This row turns to signals  $x, y : \Omega \mapsto \mathbb{R}^n$ , where  $\Omega$  now denotes a hypergraph, which is another type of topological space. This configuration is exemplified by Hypergraph Convolutional layer (Arya et al., 2020) and Hypergraph Message Passing layer (Heydari and Livi, 2022).
  - 21) **Input and output: Euclidean signal on combinatorial complex, with domain group action.** This row considers signals with the most general type of topological domain, the combinatorial complex  $\Omega$ , i.e., signals of the form  $x, y : \Omega \mapsto \mathbb{R}^n$ . Examples of neural network layers that process this type of signals are the Combinatorial Convolutions (Hajj et al., 2023b) and Combinatorial Message Passing (Hajj et al., 2023b).
  - 22) **Input and output: Euclidean signal on combinatorial complex, with domain and codomain group action.** Similar to the previous row, this last configuration process signals defined on combinatorial complex domain  $\Omega$  with Euclidean codomain. However, by contrast with the previous

row, the Euclidean codomain is equipped with a group action. The  $E(n)$ -equivariant topological neural networks from (Battiloro et al., 2024) is an example of this configuration. The layers of this network can process geometric features in the codomain  $\mathbb{R}^n$ , such as velocities or positions associated with the elements of the topological domain  $\Omega$ .

### B. Neural Network Layers with Attention

We now review mathematical structures in neural network layers that leverage the attention mechanism. In particular, we focus on how geometry, topology, and algebra can enrich the structure of the attention coefficients and the attention layers.

*Taxonomy:* Figure 8 organizes attention coefficients and layers into a taxonomy based on the mathematical properties of their inputs and outputs. First, the attention coefficient  $\alpha$  is computed from a query  $q$  and a key  $k$ . Hence, we examine the structure of the key  $k$  and the query  $q$  inputs, represented as signals over a domain. For example, the traditional transformer considers keys and queries as functions over a one-dimensional domain  $\mathbb{R}$  representing time. The output attention coefficient  $\alpha$  is represented as a signal over the product domain: in the transformer example, it is a function over the product domain  $\mathbb{R} \times \mathbb{R}$ . Second, the attention layer transforms input values  $v$  to output values  $v'$  through the attention coefficients  $\alpha$ . Hence, we look at the mathematical properties of  $v$  and  $v'$ , both represented as signals over a domain. In the classical transformers, they are signals over the time domain  $\mathbb{R}$ .

In Figure 8, we highlight the properties of the domains and codomains of the key  $k$ , query  $q$ , coefficient  $\alpha$ , input value  $v$  and output value  $v'$  signals. This graphical taxonomy helps readers understand where current methods fit within our framework and identify potential areas for innovation. We survey the field row by row in Figure 8.

#### *Geometry in Attention Mechanisms.:*

- 1) **Euclidean signal on Euclidean domain.** This row illustrates the classical transformer (Vaswani et al., 2017), with key, query, and input values represented as signals  $k, q, v : \mathbb{R} \mapsto \mathbb{R}^n$ . Attention coefficients are  $\alpha : \mathbb{R}^2 \mapsto \mathbb{R}$ , while the layer output values are  $v' : \mathbb{R} \mapsto \mathbb{R}^n$ . This row also illustrates the setting for the Vision Transformer (Dosovitskiy et al., 2021), which divides an image into a sequence of image patches: hence,

Topology, Geometry, and Algebra in Attention Mechanisms						
	Layer Input	Layer Output	Layer Operation	Layer Input	Layer Output	Layer Operation
1	$k, q : \mathbb{R} \rightarrow \mathbb{R}^n$ 	$\alpha : \mathbb{R}^2 \rightarrow \mathbb{R}$ 	Transformer [Vaswani17] Vision Transformer [Dosovitskiy21]	$k, q : P \rightarrow M$ 	$\alpha : \mathbb{R}^2 \rightarrow \mathbb{R}$ 	Geodesic [Li22]
	$v : \mathbb{R} \rightarrow \mathbb{R}^n$ 	$v' : \mathbb{R} \rightarrow \mathbb{R}^n$ 		$v : P \rightarrow \mathbb{R}^n$ 	$v' : P \rightarrow \mathbb{R}^n$ 	
2	$k, q : \mathbb{R} \rightarrow M$ 	$\alpha : \mathbb{R}^2 \rightarrow \mathbb{R}$ 	Multi-Manifold Attention [Dimitrios23]	$k, q : G \rightarrow \mathbb{R}^n$ 	$\alpha : \mathbb{R}^2 \rightarrow \mathbb{R}$ 	GAT [Veličković18]
	$v : \mathbb{R} \rightarrow \mathbb{R}^n$ 	$v' : \mathbb{R} \rightarrow \mathbb{R}^n$ 		$v : G \rightarrow \mathbb{R}^n$ 	$v' : G \rightarrow \mathbb{R}^n$ 	
3	$k, q : \mathbb{R} \rightarrow \mathbb{R}^n$ 	$\alpha : \mathbb{R}^2 \rightarrow \mathbb{R}$ 	SE(n)-Steerable Transformer [Kundu24] Geometric Algebra Transformer [Brehmer23]	$k, q : G \rightarrow \mathbb{R}^n$ 	$\alpha : \mathbb{R}^2 \rightarrow \mathbb{R}$ 	SE(3) Transformer [Fuchs20]
	$v : \mathbb{R} \rightarrow \mathbb{R}^n$ 	$v' : \mathbb{R} \rightarrow \mathbb{R}^n$ 		$v : G \rightarrow \mathbb{R}^n$ 	$v' : G \rightarrow \mathbb{R}^n$ 	
4	$k, q : M \rightarrow \mathbb{R}^n$ 	$\alpha : M^2 \rightarrow \mathbb{R}$  <small>*Here <math>M \doteq S^1</math></small>	LieTransformer [Hutchinson21]	$k, q : \Omega \rightarrow \mathbb{R}^n$ 	$\alpha : \mathbb{R}^2 \rightarrow \mathbb{R}$ 	CAN [Giusti22] SGAT [Lee22]
	$v : M \rightarrow \mathbb{R}^n$ 	$v' : M \rightarrow \mathbb{R}^n$ 		$v : \Omega \rightarrow \mathbb{R}^n$ 	$v' : \Omega \rightarrow \mathbb{R}^n$ 	Cellular Transformer [Ballester24]
5	$k, q : M \rightarrow \mathbb{R}^n$ 	$\alpha : M^2 \rightarrow \mathbb{R}$  <small>*Here <math>M \doteq S^1</math></small>	Gauge Equivariant Transformer [He21]	$k, q : \Omega \rightarrow \mathbb{R}^n$ 	$\alpha : \mathbb{R}^2 \rightarrow \mathbb{R}$ 	DHGNN [Jiang19] HyperGAT [Ding20]
	$v : M \rightarrow \mathbb{R}^n$ 	$v' : M \rightarrow \mathbb{R}^n$ 		$v : \Omega \rightarrow \mathbb{R}^n$ 	$v' : \Omega \rightarrow \mathbb{R}^n$ 	
6	$k, q : P \rightarrow \mathbb{R}^n$ 	$\alpha : \mathbb{R}^2 \rightarrow \mathbb{R}$ 	Set Transformer [Lee19] Point Cloud Transformer [Guo21]	$k, q : \Omega \rightarrow \mathbb{R}^n$ 	$\alpha : \mathbb{R}^2 \rightarrow \mathbb{R}$ 	HOAN [Hajij22]
	$v : P \rightarrow \mathbb{R}^n$ 	$v' : P \rightarrow \mathbb{R}^n$ 		$v : \Omega \rightarrow \mathbb{R}^n$ 	$v' : \Omega \rightarrow \mathbb{R}^n$ 	

**Fig. 8: Topology, Geometry, and Algebra in Attention Mechanisms** categorized according to the mathematical properties of the attention coefficients (first subrow of each row) and of the attention layer (second subrow of each row). The key  $k$  and the query  $q$  are the inputs to the attention coefficient  $\alpha$ ; the value  $v$  is the input to the attention layer, and the output value  $v'$  is the weighted result of that layer. Inputs and outputs are represented as signals, i.e., as functions from a domain to a codomain. The black curved arrows represent the action of a group on a signal's domain or codomain. Notations:  $\mathbb{R}^n$ : Euclidean space;  $M$ : Manifold;  $P$ : point set;  $G$ : graph;  $\Omega$ : topological space.

patches in  $\mathbb{R}^n$  over  $\mathbb{R}$ . We highlight the difference between the mathematical representation of these signals, and their computational representation during an actual implementation of the transformer. Mathematically, we represent the signals' domain as the continuous real line  $\mathbb{R}$ . Computationally, however, this real line is discretized into  $T$  steps and associated  $T$  discrete tokens (for either words or image patches). Yet, the representation as the real line is useful to unify the original transformer with the more complicated layers introduced next.

- 2) **Manifold signal on Euclidean domain for keys and queries.** Compared to the classical transformer of the previous row, this row introduces geometry in the codomains of the keys and query signals, which write  $k, q : \mathbb{R} \mapsto M$ . Meanwhile, the attention coefficients  $\alpha$ , the input and output values  $v, v'$  have the same structure as in the classic transformer. The multimanifold attention mechanisms by (Konstantinidis et al., 2023) illustrates this configuration. Specifically, this work considers the classical attention coefficient  $\alpha$  as the computation of a Euclidean distance between key and query. Accordingly, their proposed geometric attention coefficient replaces the Euclidean distance by a Riemannian geodesic distance between key and query, which are interpreted as elements of a manifold: the manifold of SPD (symmetric positive definite) matrices, the Grassmann manifold, or both—hence the term “multi”-manifold. We note that the input data to this transformer architecture is still Euclidean, since this attention mechanism is proposed for images in vision transformers. However, the way this data is processed by the transformer's internal layers is non-Euclidean.

*Equivariance in Attention Mechanisms.:*

- 3) **Euclidean signal on Euclidean domains for keys, queries and values, with group action on codomain.** This row illustrates an attention mechanism that includes additional algebraic structure in both keys, queries, input and output values. The Geometric Algebra Transformer represents this configuration Brehmer et al. (2023). Its layers were designed to process “geometric data” defined as scalars, vectors, lines, planes, objects and their transformations (e.g., rotations) in 3D space. Such geometric data is encoded into multivectors, which are elements of the projective geometric algebra also called the Clifford algebra. For simplic-

ity, we consider this space as a Euclidean space  $\mathbb{R}^n$  with algebraic structure. The attention coefficients are group invariant, while the attention layer is group equivariant, for the Euclidean group  $E(3)$  of translations, rotations and reflections in 3D space. This configuration is also illustrated by the Steerable Transformer (Kundu and Kondor, 2024) which processes Euclidean codomains  $\mathbb{R}^n$  with equivariance to the special Euclidean group  $SE(n)$ , for application to image processing and machine learning tasks.

- 4) **Euclidean signal on manifold domain for all inputs / outputs, with domain group action.** Similar to the previous row, this row also introduces geometric structure in the keys, queries, values. In contrast to the previous row, however, this layer brings geometry into the domains of the signals:  $k, q, v, v'$  whereas the above layer brought geometry in their codomains. Consequently, for this row, the attention coefficients  $\alpha : M \times M \mapsto \mathbb{R}$  have the product manifold  $M \times M$  as their domains. This configuration is illustrated in the Lie Transformer (Hutchinson et al., 2020), where the manifolds of interest are Lie groups and their subgroups. We note that the data processed by this architecture does not have to belong to a Lie group; only to be acted upon by a Lie group. A lifting layer is introduced to convert the raw data into Lie group elements, which are then handled by the Lie Transformer. The attention layer is then equivariant.
- 5) **Euclidean signals on manifold domains for all inputs / outputs.** This row is similar to the previous row, using manifold domains for keys, queries, values, and attention coefficients. By contrast with the previous row, the group equivariance is replaced by the concept of gauge equivariance and invariance. The Gauge invariant transformer in He et al. (2021) presents such configuration: the attention coefficients are gauge invariant, and the attention layer is gauge equivariant. This work exclusively focuses on two-dimensional manifolds  $M$  embedded in 3D Euclidean space.

*Topology in Attention Mechanisms.:*

- 6) **Euclidean signal on set domain, with domain group action:** This row introduces topological structure on the domains of the signals  $k, q, v, v' : P \mapsto \mathbb{R}^n$ , through the set of points  $P$ . The Set Transformer (ST) (Lee et al., 2019) and the Point Cloud Transformer (PCT) (Guo et al., 2021) are two examples of this configuration. They enjoy

equivariance to the group of permutations, which acts by permuting the indexing of the points in the set (resp., in the point cloud).

- 7) **Manifold signals on set domains, with domain group action.** This row includes geometric structure on top of the topological structure of the previous row, using manifold codomains for keys  $k$ , queries  $q$  and Euclidean signals for  $v$  and  $v'$ , all on set domains. The geodesic transformer (Li et al., 2022b) provides an architecture that processes this configuration. Similar to the Multi-Manifold Attention of row 2, the attention coefficient of the geodesic transformer is computed using a geodesic distance between keys and queries: either a graph-based geodesic distance, or a Riemannian geodesic distance on the so-called oblique manifold.
- 8) **Euclidean signals on graph domain, with domain group action.** This row is similar to the previous row, but without a group action on the signals codomains. This is illustrated in the Graph Attention Transformer (GAT) (Veličković et al., 2018).
- 9) **Euclidean signals on graph domains, with domain and codomain group actions.** This row also uses a graph domain  $G$  such that  $k, q, v, v' : G \mapsto \mathbb{R}^n$ . An example of this configuration is the  $SE(3)$ -Transformer, where the codomain of these signals is additionally restricted to  $\mathbb{R}^3$ , equipped with an action of the group of translations and rotations in 3D  $SE(3)$  (Fuchs et al., 2020). This transformer was proposed to process 3D point clouds, and provides  $SE(3)$ -invariant attention coefficients and  $SE(3)$ -equivariant attention layer.
- 10) **Euclidean signals on cellular complex domain, with domain group action.** Starting on this row, more complicated topological structure is introduced on the domains  $\Omega$  of the signals. We refer the reader to the survey (Papillon et al., 2023) for a detailed exposition of the attention mechanisms using topology. This row presents architectures that specifically use a cellular complex or a simplicial complex as the domain. Cell Attention Networks (CAN) (Giusti et al., 2023) and Simplicial Graph Attention Network (SGAT) (Lee et al., 2022) illustrate this type of attention mechanism, while the Cellular Transformer (Ballester et al., 2024) additionally include positional encodings.
- 11) **Euclidean signals on hypergraph domain, with**

**domain group action.** Similar to the previous row, this configuration uses topological structure on the domains of the signals: here, leveraging hypergraphs. Examples of this configuration include Dynamic Hypergraph Neural Networks (DHGNN) (Jiang et al., 2019) and Hypergraph Attention Networks (Hyper GAT) (Ding et al., 2020).

- 12) **Euclidean signals on combinatorial complex domain, with domain group action.** This final row uses a combinatorial complex domain for the signals defining inputs of the attention coefficients and attention layers. A Higher Order Attention Network (HOAN) architecture is a recent example of this last category (Hajj et al., 2023b).

### C. Benchmarks

We now turn to a brief review of the benchmarks that have been considered in the non-Euclidean deep learning literature, compiling results from a broad sample of neural networks with topological, geometric, and algebraic layers in Table I, and highlighting the diversity of tasks and datasets used in the literature.

*Tasks and Datasets:* We first observe that a wide variety of task and benchmark datasets have been used in the literature, with little overlap between models. In other words, it is rare that two different models have been benchmarked on the same dataset. This is not surprising, since different models use different geometric, topological, and algebraic structures and different structures are well suited for different tasks.

There are, however several benchmarks that appear across models: MNIST and CIFAR for image classification, and Cora, Citeseer, and Pubmed for graph classification. Many geometrical models are tested by examining how well they model dynamical or physical systems. These results are not easily comparable across models, as the tasks are often customized for each paper.

*Number of parameters:* A key benefit of building mathematical structure into neural networks is that it constrains the hypothesis search space. If the structure is well matched to the problem, the model should require fewer parameters and fewer computations. Many papers mention this, but only a few report the number of parameters (see right column of Table I). As parameter and data efficiency are frequently cited as advantages of building structure into neural network models, we encourage authors to more regularly report

**TABLE I: Applications and Benchmark of Neural Networks with Geometric, Topological and Algebraic Structures.**

We organize models according to whether it uses attention and their geometric, topological and algebraic structure, with the abbreviations: M: manifold,  $G_p$ : group,  $S$ : set,  $G$ : graph,  $\Omega$ : topological domain,  $A$ : algebra. Models are also organized based on which task they perform, and on which benchmark datasets. We include accuracies for benchmarks that two or more models use, converting test error to accuracy when needed, along with standard error if reported. Model parameters are listed if the paper reports them. N. R. means Not Reported.

	Model	Structure	Task	Benchmark datasets	# Params
Without Attention	Riemannian VAE <a href="#">Miolane19</a>	M	Dimension Reduction	Human Connectome Project (HCP)	N.R.
	S-VAE/VGAE <a href="#">Davidson18</a>	M	Latent representation for image classification and link prediction	MNIST (93.4± 0.2*), Cora (94.1±0.3), Citeseer (95.2±0.2), Pubmed (96.0±0.1)	N.R.
	SPDNet <a href="#">Huang, VanGool16</a>	M	Visual classification (emotion, action, face)	AFEW, HDM05 and PaSC	N.R.
	EMLP <a href="#">Finzi21</a>	$G_p$	Dynamical modeling	Double pendulum	N.R.
	LeNet-5 <a href="#">LeCun98</a>	$G_p$	Image classification	MNIST (99.2±0.1)	N.R.
	Steerable CNN <a href="#">Cohen, Welling17</a>	$G_p$	Image classification	CIFAR (10: 76.3; 10+: 96.4; 100+: 81.2)	4.4M 9.1M
	G-CNN <a href="#">Cohen, Welling16</a>	$G_p$	Image classification	Rotated MNIST, CIFAR (10: 93.5; 10+: 95.1)	2.6M
	G-CNN <a href="#">Cohen19a</a>	$G_p$	Climate, pointcloud segmentation	Climate Segmentation, Stanford 2D-3D-S	N.R.
	E(n)-EGNN <a href="#">Satorras2021</a>	$G_p$	Molecular property prediction, dynamical modeling	QM9, N-body, Graph autoencoder	N.R.
	PONITA <a href="#">Bekkers2024</a>	$G_p$	Molecular property prediction and generation, dynamical modeling	rMD17, QM9, N-body	N.R.
	PointNet++ <a href="#">Qi17</a>	S	Image, 3D, scene classification	MNIST (99.49), ModelNet40 (91.9), SHREC15, ScanNet	1.7M
	Tensor field network <a href="#">Thomas18</a>	S	3D-point-cloud prediction	QM9	N.R.
	GCN <a href="#">Kipf, Welling17</a>	G	Link prediction	Cora, Citeseer, Pubmed, NELL	N.R.
	enn-s2s <a href="#">Gilmer17</a>	G	Molecular property prediction	QM9	N.R.
	SNN <a href="#">Ebli20</a>	$\Omega$	Coauthorship prediction	Semantic Scholar Open Research Corpus	N.R.
	MPSN <a href="#">Bodnar21</a>	$\Omega$	Trajectory, graph classification	TUDataset	N.R.
	CXN <a href="#">Hajij20</a>	$\Omega$	-	-	N.R.
	HMPNN <a href="#">Heydari22</a>	$\Omega$	Citation node classification	Cora (92.2)	N.R.
	CCNN <a href="#">Hajij23</a>	$\Omega$	Image segmentation, image, mesh, graph classification	Human Body, COSEG, SHREC11	N.R.
	E(n)-EMPSN <a href="#">Eijkelboom2023</a>	$\Omega$	Molecular property prediction, dynamical modeling	QM9, N-body	200K
	Clifford-EMPSN <a href="#">Liu2024</a>	$\Omega$	Pose estimation, dynamical modeling	CMU MoCap, MD17	200K
	E(n) Equivariant TNN <a href="#">Battiloro2024</a>	$\Omega$	Molecular property, air pollution prediction	QM9, Air Pollution Downscaling	1.5M
	With Attention	Transformer <a href="#">Vaswani17</a>	-	Machine translation	WMT 2014
MMA ViT <a href="#">Konstantinidis23</a>		M	Image classification, segmentation	CIFAR (10: 94.7, 100+: 77.5), T-ImageNet, ImageNet, ADE20K	3.9M
GATr <a href="#">Brehmer23</a>		A	Dynamical modeling	N-body, artery stress, diffusion robotics	4.0M
Steerable Transformer <a href="#">Kundu2024</a>		$G_p$	Point-cloud, Image classification	Rotated MNIST (99.03), ModelNet10 (90.4)	0.9M
Lie Transformer <a href="#">Hutchinson20</a>		$G_p$	Regression, dynamics	QM9, ODE spring simulation	0.9M
GET <a href="#">He21</a>		M	Shape classification, segmentation	SHREC07, Human Body Segmentation	0.15M
Set Transformer <a href="#">Lee19</a>		S	Max value regression, clustering	Omniglot, CIFAR (100: 0.92±0.01)	N.R.
PCT <a href="#">Guo21</a>		S	Point-cloud classification, regression, segmentation	ModelNet40 (93.2), ShapeNet (86.4), S3DIS	1.4M
GSA <a href="#">Li22</a>		S	Object classification, segmentation	ModelNet40 (93.3), ScanObjectNN, ShapeNet (85.9)	18.5M
SE(3)-Transformer <a href="#">Fuchs20</a>		G	Dynamics, classification, regression	N-body, ScanObjectNN, QM9	N.R.
GAT <a href="#">Veličković18</a>		G	Link prediction	Cora, Citeseer, Pubmed, PPI	N.R.
CAN <a href="#">Giusti23</a>		$\Omega$	Graph classification	TUDataset	N.R.
Cellular Transformer <a href="#">Ballester24</a>		$\Omega$	Graph classical, Graph regression	GCB, Zinc, Ogbg Molhiv	N.R.
SGAT <a href="#">Lee22</a>		$\Omega$	Node classification	DBLP <sup>2</sup> , ACM, IMDB	N.R.
DHGNN <a href="#">Jiang19</a>		$\Omega$	Link, sentiment prediction	Cora (82.5), Microblog	0.13M
HyperGAT <a href="#">Ding20</a>	$\Omega$	Text classification	20NG, R8, R52, Ohsumed, MR	N.R.	

parameter counts and computational cost in their papers along with performance metrics.

#### D. Summary

This concludes our review on non-Euclidean in deep neural network layers. While a great diversity of structures, layer types, and mechanisms have been proposed, we hope that our illustrated taxonomy may aid researchers in understanding their differences and similarities, and in identifying opportunities for innovation and application. We now turn to a brief summary of the existing software libraries for non-Euclidean machine learning made available online, and end with an overview of the domains in which non-Euclidean ML methods have been applied.

## VI. NON-EUCLIDEAN SOFTWARE

In this section, we highlight publicly available software libraries that make the methods of this field computationally accessible, organized in Table II. Here, we limit our discussion to libraries whose commit history suggests continued development and have a following indicated by at least 50 Github Stars.

Table II highlight libraries core to the field. As shown by the number of stars and actively developed repositories, packages for topological methods are the most well developed, including important engineering foundations such as CUDA and C++ accelerated network primitives, and large collections of model implementations that continue to be maintained. The library ecosystem for geometric learning methods is quickly growing in interest and contributors, extending the packages beyond optimizers over specific manifolds to more general differential geometry tools. While the packages for algebra in machine learning are the most nascent, there have been exciting new developments within the past few years in making more specialized packages for accelerating group convolutions and other algebraic operations as the need for more specialized applications have emerged.

## VII. APPLICATIONS OF NON-EUCLIDEAN GEOMETRY

Many problems in science and engineering are intrinsically non-Euclidean and thus provide an exciting

opportunity for the application of non-Euclidean ML methods. Here, we briefly highlight key developments in selected application areas. We refer the reader to Bronstein et al. (2021), Gaudelet et al. (2021), Li et al. (2022a), Rajpurkar et al. (2022), Wang et al. (2023), Wu et al. (2022, 2021) for more comprehensive discussions of applications.

### Chemistry and Drug Development

Within computational chemistry, molecular analysis and design are traditionally lengthy and expensive processes, sometimes requiring decades of development time, and billions of dollars of investment and infrastructure. Molecular data inherently has geometric and graphical structure, well suited for non-Euclidean approaches (Atz et al., 2021).

Graph neural networks have become a workhorse for molecular analysis, treating molecules as graphs with atoms as nodes and bonds as edges (Bronstein et al., 2021, Gilmer et al., 2017). Progress in this field has largely involved the construction of message-passing neural networks with favorable properties, such as equivariance to a growing family of group transformations, novel forms of weight sharing, more expressive primitives, and more efficient formulations for parameterization and computation (Batzner et al., 2022, Bekkers et al., 2024, Satorras et al., 2022, Schütt et al., 2017, Thomas et al., 2018). Deep networks with geometric structure have also been used directly for drug screening to discover new antibiotics (Stokes et al., 2020).

Recently, deep equivariant generative modeling has emerged as a powerful framework for molecule synthesis. Prior work by (Gebauer et al., 2020, Simm et al., 2020, Simonovsky and Komodakis, 2018) establishes the importance of leveraging geometric properties for the synthesis of molecules. (Hoogeboom et al., 2022) introduces equivariant denoising diffusion models for molecule generation by directly generating 3D atomic coordinates, demonstrating improved quality and efficiency. This was recently extended by (Xu et al., 2023) to perform equivariant diffusion over a molecular latent space, and by (Vignac et al., 2023) which achieves much higher stability for generated molecules on the GEOM-DRUGS dataset. Another line of work generates molecular invariants such as angles and distances, which then are used to produce coordinates (Luo and Ji, 2022). Recent work has also demonstrated the importance of equivariances and invariances for molecular conformer generation (Reidenbach and Kr-

ishnapriyan, 2023, Xu et al., 2022).

### Structural Biology and Protein Engineering

Proteins are 1D sequences of amino acids that fold into a 3D structure. The function of a protein is defined by its structure, so the prediction of protein structure from the original 1D sequence is crucial to the analysis of their uses and interactions with other biomolecules. AlphaFold 2, which incorporates a graph-structured backbone, equivariant attention, and many geometric priors about molecules (Jumper et al., 2021), has emerged as a landmark paper for predicting protein structure. Such protein structure predictions are commonly utilized for applications in biology and medicine (Yang et al., 2023). Prediction of the interactions of proteins with other molecules is also a challenging problem well represented by graphs and equivariant methods (Anand and Achim, 2022, Ingraham et al., 2023, 2019).

### Computer Vision

Computer vision entails the inference of properties of the visual world from images or other measurements such as LIDAR. There are many sub-tasks in computer vision such as object recognition, semantic segmentation, image and video generation, depth estimation, etc. Historically, network primitives that capture the topological structure and symmetries of images have dominated vision benchmarks, including CNNs, GCNNs, and Vision transformers (Cohen and Welling, 2016, Dosovitskiy et al., 2021, Krizhevsky et al., 2012, LeCun et al., 1998).

Recently, one of the most successful applications of non-Euclidean deep learning has been that of graph neural networks, implemented on data native to or lifted to point-clouds. Pioneering works such as Pointnet++ and PointTransformer introduced graph-structured deep networks as breakthrough methods in 3D semantic segmentation and object detection at whole-room scales (Engel et al., 2020, Qi et al., 2017). Another promising computational primitive, Slot Attention, introduces a novel messaging-passing strategy to perform unsupervised object discovery using permutation invariant slots, which incorporates spatial symmetries using slot-centric reference frames (Biza et al., 2023, Locatello et al., 2020).

### Biomedical Imaging

Biomedical imaging involves inferring the structure of biological tissues from measurements of their physical properties, typically in the form of electromagnetic fields, acoustic waves, and other physical phenomena.

Quantities of interest include shape, composition, or internal state. Thus, geometric and topological structure play an important role in their analysis.

Many machine learning problems in medical imaging require reasoning about 3D structures, including their shape, their variations throughout a population, and changes throughout time. As tissue states are non-Euclidean, their statistics and evolution require a geometric treatment (Pennec et al., 2019). Variations in organ shapes lie on low-dimensional manifolds, and geometry-aware dimensionality-reduction methods such as tangent PCA (Boisvert et al., 2008) or Principle Geodesic Analysis (PGA) enable meaningful representations for downstream tasks (Fletcher and Joshi, 2007, Fletcher et al., 2004, Hinkle et al., 2012a). Geometric methods have been applied to the analysis of the effects of aging in the corpus collosum with MRI scans (Hinkle et al., 2012b), to brain connectomics data in Diffusion Tensor Imaging (Pennec et al., 2006), and to the segmentation of 3D anatomical structures from CT and MRI scans in the lateral cerebral ventricle, the kidney parenchyma and pelvis, and the hippocampus (Pizer et al., 2003).

Medical image registration has historically steered the need for the development of statistics on Lie groups from the finite-dimensional group  $SE(3)$  (Pennec, 2006, Pennec and Thirion, 1997) to the infinite-dimensional group of diffeomorphisms (Trounev, 1998, Younes, 2010). Unfortunately, any attempt to rely on Riemannian geometric structures for machine learning on Lie groups is generally ill-posed. Specifically, classical Riemannian metrics on Lie groups, called left or right invariant, generally fail to be invariant by all the group operations, notably inversion. This triggered the search for alternative geometric structures (Miolane and Pennec, 2015, Pennec and Arsigny, 2012) and the replacement of the (non bi-invariant) Riemannian metric by the canonical bi-invariant symmetric Cartan-Shouten connection Pennec and Lorenzi (2020). In infinite dimensions, this grounds the parametrization of diffeomorphisms by the flow of Stationary Velocity Fields (SVFs). This geometrically grounded statistical framework on Lie groups is now used in numerous non-linear medical image registration algorithms (Arsigny et al., 2006, Lorenzi and Pennec, 2013) and to model shape evolution such as the brain changes in Alzheimer's disease (Hadj-Hamou et al., 2016, Lorenzi et al., 2015, Sivera et al., 2019).

In medical image segmentation, estimation errors on the order of a few pixels can lead to significant misinterpretations. The domain has recently seen benefits

### Geometry

Packages	Domains	Core Features	Stars
GeomStats <a href="#">2019</a>	Manifolds, Lie Groups, Fiber Bundles, Shape Spaces, Information Manifolds, Graphs	Manifold operations, Algorithms, Statistics, Optimizers	1.2k
GeoOpt <a href="#">2020</a>	Manifolds	Layers, Manifold operations, Stochastic optimizers for deep learning	812
PyManOpt <a href="#">2016</a>	Manifolds, Lie Groups	Manifold operations, Optimizers	734
PyRiemann <a href="#">2023</a>	SPD Matrices	Machine Learning, Data Analysis for biosignals	606

### Topology

Packages	Domains	Core Features	Stars
PytorchGeometric <a href="#">2019</a>	Graphs	Baseline Models, Layers, Fast Basic Graph Operations, Datasets, Dataloaders	20.6k
NetworkX <a href="#">Hagberg et al. (2008)</a>	Graphs, Digraphs, Multigraphs	Data structures, Graph generators, Graph Algorithms, Network Analysis Measures	14.5k
DGL <a href="#">2019</a>	Graphs	Baseline Models, Layers, Fast Basic Graph Operations, Datasets, Dataloaders, Framework-agnostic (PyTorch, Tensorflow, etc. are swappable)	13.2k
DIG <a href="#">2021</a>	Graphs	Baseline models, Datasets, Evaluation Metrics	1.8k
AutoGL <a href="#">2021</a>	Graphs	Neural Architecture Search, Hyper-Parameter Tuning, Ensembles	1.1k
HyperNetX <a href="#">2023</a>	Hypergraphs	Machine Learning Algorithms, Analysis, Visualization	502
DHG <a href="#">2022</a>	Graphs, hypergraphs, bipartite graphs, hypergraphs, directed hypergraphs, ...	Models, Basic Operations, Dataloaders, Visualization, Auto ML, Metrics, Graph generators	566
TopoModelX <a href="#">2024</a>	Graphs, colored hypergraphs, complexes	Baseline Models, Layers, Higher-order message passing	205
TopoNetX <a href="#">2024</a>	Graphs, colored hypergraphs, complexes	Topography Generators, Computing topological properties, Arbitrary cell attributes	168
TopoEmbedX <a href="#">2024</a>	Graphs, colored hypergraphs, complexes	Representation learning, embeddings	72
TopoBenchmarkX <a href="#">2024</a>	Graphs, hypergraphs, complexes	Benchmarks, lifting, dataloaders, losses, training framework	54
XGI <a href="#">2023</a>	Hypergraphs, directed hypergraphs, symplical complexes	Graph generators, metrics, algorithms, dataloaders, visualization	172

### Algebra

Packages	Domains	Core Features	Stars
E3NN <a href="#">2022</a>	E(3) Equivariant Feature Fields	Group Convolutions, Steerable Group Convolutions	891
ESCNN & E2CNN <a href="#">2022</a>	E(n) Equivariant Feature Fields, Graphs	Group Convolutions, Steerable Group Convolutions	584 <sup>1</sup>
NequIP <a href="#">2022</a>	E(3) Equivariance on Graphs	Group Convolutions, Steerable Group Convolutions	538
EMLP <a href="#">2021</a>	Matrix Groups, Tensors, Irreducible Representations, Induced Representations	Programmatic generation of equivariant MLPs for arbitrary matrix groups in JAX	249
PyQuaternion	Quaternions	Quaternion operations, rotation representation conversions, differentiation, integration	336

**TABLE II: Software Packages for Machine Learning with Topology, Geometry, and Algebra.** We organize packages according to the mathematical, non-Euclidean structures they focus on.

from the addition of topological structure. Examples of topological constraints that improve consistency and accuracy include preserving membrane connectivity for cell images and incorporating anatomically correct relative position of organs (Clough et al., 2022, Gupta et al., 2022, Hu et al., 2019, 2021).

Cryo-EM data provide multiple 2D image projections of a 3D biomolecule from different angles. The task of inferring the original 3D structure of a biomolecule benefits greatly from the incorporation of topological and geometric structure (Donnat et al., 2022, Miolane et al., 2020).

Histology images have no canonical orientation, meaning each orientation of a particular cell is equally likely to appear. Recent works have explored equivariant and steerable CNNs to leverage these symmetries in the data (Adnan et al., 2020, Bekkers et al., 2018, Graham et al., 2020, Lafarge et al., 2020, Veeling et al., 2018)

### Recommender Systems and Social Networks

Recommender systems were one of the first successful applications of graph representation learning, where the proximity of a particular node to other nodes can be learned through graph convolutions to represent similarity. This has clear economic utility for recommending advertisements, products, music, and content based on the user’s data and preferences. PinSage from Pinterest was one of the first to demonstrate their potential at a commercial scale (Ying et al., 2018). See (Wu et al., 2022) for a comprehensive review on graph neural networks in recommender systems.

### Physics

Physics data naturally has many symmetries and often takes the form of relations between unordered sets, an ideal setting for topological and equivariant methods. Dynamics between particles or nodes in a mesh can be effectively computed using learned graph message passing for various types of physics data (Pfaff et al., 2021, Sanchez-Gonzalez et al., 2020). Equivariant transformer and graph neural network architectures have been successfully applied to data analysis for the Large Hadron Collider and other simulations such as gravity for the n-body problem (Brandstetter et al., 2022, Fuchs et al., 2020). Topological methods are well suited to process the hundreds of petabytes of highly relational data produced by experiments from the Large Hadron Collider and have demonstrated their utility for the next stage of fundamental discoveries in particle physics (DeZoort et al., 2023). Recent work (Brehmer

et al., 2023) proposes an architecture for embedding geometric data into a Geometric Algebra representation to be processed by an equivariant Transformer network, and demonstrates its efficacy on mesh interaction estimation and n-body simulation. Astrophysics data is also well suited for application of equivariant networks. Some examples include the classification of radio galaxies using group-equivariant CNNs (Scaife and Porter, 2021), optimal cosmological analysis using equivariant normalizing flows (Dai and Seljak, 2022), and cosmic microwave background radiation analysis using spherical equivariant CNNs (McEwen et al., 2022).

### Other Applications

There are many other interesting applications of non-Euclidean methods to domains that do not neatly fall into these categories, such as GNNs for arrival time forecasting (Derrow-Pinion et al., 2021), weather forecasting (Keisler, 2022, Lam et al., 2023), materials science (Reiser et al., 2022), patient electronic health records (Li et al., 2022a), and many more. As a burgeoning young field, the application of non-Euclidean machine learning to novel domains is constantly advancing. We expect (and hope) that the highlights presented here will represent only a small fraction of what is to come.

## VIII. CONCLUSION

As the availability of richly structured, non-Euclidean data grows across application domains, there is an increasing need for machine learning methods that can fully leverage the underlying geometry, topology, and symmetries to extract insights. Driven by this need, a new paradigm of non-Euclidean machine learning is emerging that generalizes classical techniques to curved manifolds, topological spaces, and group-structured data. This paradigm shift echoes the non-Euclidean revolution in mathematics in the 19th century, which radically expanded our notion of geometry and catalyzed significant advancements across the natural sciences.

In this review, we have provided an accessible overview of this emerging field, unifying disparate threads in the literature into a common organizational framework. Our illustrated taxonomy contextualizes, classifies, and differentiates existing approaches and illuminates gaps that present opportunities for innovation. We hope this serves as an invitation for both theoreticians and practitioners to further explore the potential of non-Euclidean geometry, topology, and algebra to reshape modern machine learning, just as

they reshaped our fundamental understanding of space over a century ago.

By empowering models with the tools to respect the underlying structure of data, non-Euclidean machine learning greatly expands the frontiers of the types of learning problems that can be tackled. With a growing theoretical understanding and the design of architectures that fully leverage the mathematical formalisms of geometry, topology and algebra, non-Euclidean approaches hold immense potential to transform the broader machine learning landscape and its application to engineering problems and the natural sciences in the coming years.

## REFERENCES

- Mohammed Adnan, Shivam Kalra, and Hamid R. Tizhoosh. Representation learning of histopathology images using graph neural networks, 2020.
- Morten Akhøj, James Benn, Erlend Grong, Stefan Sommer, and Xavier Pennec. Principal subbundles for dimension reduction. working paper or preprint, July 2023. URL <https://inria.hal.science/hal-04156036>.
- Namrata Anand and Tudor Achim. Protein structure and sequence generation with equivariant denoising diffusion probabilistic models, 2022.
- Vincent Arsigny, Olivier Commowick, Xavier Pennec, and Nicholas Ayache. A Log-Euclidean Framework for Statistics on Diffeomorphisms. In *Proc. of the 9th International Conference on Medical Image Computing and Computer Assisted Intervention (MICCAI'06), Part I*, LNCS, pages 924–931, October 2006. doi: 10.1007/11866565\_113.
- Devanshu Arya, Richard Olij, Deepak K. Gupta, Ahmed El Gazzar, Guido van Wingen, Marcel Worring, and Rajat Mani Thomas. Fusing structural and functional mris using graph convolutional networks for autism classification. In Tal Arbel, Ismail Ben Ayed, Marleen de Bruijne, Maxime Descoteaux, Herve Lombaert, and Christopher Pal, editors, *Proceedings of the Third Conference on Medical Imaging with Deep Learning*, volume 121 of *Proceedings of Machine Learning Research*, pages 44–61. PMLR, 06–08 Jul 2020. URL <https://proceedings.mlr.press/v121/arya20a.html>.
- Kenneth Atz, Francesca Grisoni, and Gisbert Schneider. Geometric deep learning on molecular representations, 2021.
- Rubén Ballester, Pablo Hernández-García, Mathilde Papillon, Claudio Battiloro, Nina Miolane, Tolga Birdal, Carles Casacuberta, Sergio Escalera, and Mustafa Hajji. Attending to topological spaces: The cellular transformer. *arXiv preprint arXiv:2405.14094*, 2024.
- Monami Banerjee, Rudransh Chakraborty, Edward Ofori, David Vailancourt, and Baba C. Vemuri. *Nonlinear Regression on Riemannian Manifolds and Its Applications to Neuro-Image Analysis*, page 719–727. Springer International Publishing, 2015. ISBN 9783319245539. doi: 10.1007/978-3-319-24553-9\_88. URL [http://dx.doi.org/10.1007/978-3-319-24553-9\\_88](http://dx.doi.org/10.1007/978-3-319-24553-9_88).
- Alexandre Barachant, Quentin Barthélemy, Jean-Rémi King, Alexandre Gramfort, Sylvain Chevallier, Pedro L. C. Rodrigues, Emanuele Olivetti, Vladislav Goncharenko, Gabriel Wagner vom Berg, Ghiles Reguig, Arthur Lebeurier, Erik Bjäreholt, Maria Sayu Yamamoto, Pierre Clisson, and Marie-Constance Corsi. *pyriemann/pyriemann: v0.5*, 2023. URL <https://doi.org/10.5281/zenodo.8059038>.
- Claudio Battiloro, Ege Karaismailoğlu, Mauricio Tec, George Dasoulas, Michelle Audirac, and Francesca Dominici. E(n) equivariant topological neural networks. *arXiv preprint arXiv:2405.15429*, 2024.
- Simon Batzner, Albert Musaelian, Lixin Sun, Mario Geiger, Jonathan P Mailoa, Mordechai Kornbluth, Nicola Molinari, Tess E Smidt, and Boris Kozinsky. E(3)-equivariant graph neural networks for data-efficient and accurate interatomic potentials. *Nature communications*, 13(1):2453, 2022.
- Erik J Bekkers, Maxime W Lafarge, Mitko Veta, Koen AJ Eppenhof, Josien PW Pluim, and Remco Duits. Roto-translation covariant convolutional networks for medical image analysis, 2018.
- Erik J Bekkers, Sharvaree Vadgama, Rob D Hesselink, Putri A van der Linden, and David W Romero. Fast, expressive se(n) equivariant networks through weight-sharing in position-orientation space, 2024.
- Andri Bergsson and Søren Hauberg. Visualizing riemannian data with rie-sne. *arXiv preprint arXiv:2203.09253*, 2022.
- Charles M. Bishop. Bayesian pca. In *Neural Information Processing Systems*, 1998. URL <https://api.semanticscholar.org/CorpusID:43329106>.
- Ondrej Biza, Sjoerd van Steenkiste, Mehdi S. M. Sajjadi, Gamaleldin F. Elsayed, Aravindh Mahendran, and Thomas Kipf. Invariant slot attention: Object discovery with slot-centric reference frames, 2023.
- Cristian Bodnar. *Topological Deep Learning: Graphs, Complexes, Sheaves*. PhD thesis, 2023.
- Cristian Bodnar, Fabrizio Frasca, Yuguang Wang, Nina Otter, Guido F Montufar, Pietro Lió, and Michael Bronstein. Weisfeiler and lehman go topological: Message passing simplicial networks. In Marina Meila and Tong Zhang, editors, *Proceedings of the 38th International Conference on Machine Learning*, volume 139 of *Proceedings of Machine Learning Research*, pages 1026–1037. PMLR, 18–24 Jul 2021. URL <https://proceedings.mlr.press/v139/bodnar21a.html>.
- Jonathan Boisvert, Farida Cheriet, Xavier Pennec, Hubert Labelle, and Nicholas Ayache. Geometric Variability of the Scoliotic Spine using Statistics on Articulated Shape Models. *IEEE Transactions on Medical Imaging*, 27(4):557–568, 2008. doi: 10.1109/TMI.2007.911474.
- G. E. P. Box and G. C. Tiao. A bayesian approach to some outlier problems. *Biometrika*, 55(1):119–129, 1968. ISSN 1464-3510. doi: 10.1093/biomet/55.1.119. URL <http://dx.doi.org/10.1093/biomet/55.1.119>.
- Johannes Brandstetter, Rob Hesselink, Elise van der Pol, Erik J Bekkers, and Max Welling. Geometric and physical quantities improve e(3) equivariant message passing, 2022.
- Johann Brehmer, Pim De Haan, Sönke Behrends, and Taco Cohen. Geometric algebra transformer. In *Thirty-seventh Conference on Neural Information Processing Systems*, 2023. URL <https://openreview.net/forum?id=M7r2CO4JJC>.
- Leo Breiman. *Machine Learning*, 45(1):5–32, 2001. ISSN 0885-6125. doi: 10.1023/a:1010933404324. URL <http://dx.doi.org/10.1023/A:1010933404324>.
- Michael M Bronstein, Joan Bruna, Taco Cohen, and Petar Veličković. Geometric deep learning: Grids, groups, graphs, geodesics, and gauges. *arXiv preprint arXiv:2104.13478*, 2021.
- Gabriele Cesa, Leon Lang, and Maurice Weiler. A program to build E(N)-equivariant steerable CNNs. In *International Conference on Learning Representations (ICLR)*, 2022.
- Rudransh Chakraborty, Jose Bouza, Jonathan H. Manton, and Baba C. Vemuri. ManifoldNet: A Deep Neural Network for Manifold-Valued Data With Applications. *IEEE Transactions on Pattern Analysis and Machine Intelligence*, 44(2):799–810, February 2022. ISSN 0162-8828, 2160-9292, 1939-3539. doi: 10.1109/TPAMI.2020.3003846. URL <https://ieeexplore.ieee.org/document/9122448/>.
- Kui Yu Chang and Joydeep Ghosh. A unified model for probabilistic principal surfaces. *IEEE Transactions on Pattern Analysis and Machine Intelligence*, 23(1):22–41, 2001. ISSN 01628828. doi: 10.1109/34.899944.
- Nikolai Chernov. *Circular and Linear Regression: Fitting Circles and Lines by Least Squares*. CRC Press, June 2010. ISBN 9780429151415. doi: 10.1201/ebk1439835906. URL

- <http://dx.doi.org/10.1201/EBK1439835906>.
- James R. Clough, Nicholas Byrne, Ilkay Oksuz, Veronika A. Zimmer, Julia A. Schnabel, and Andrew P. King. A topological loss function for deep-learning based image segmentation using persistent homology. *IEEE Transactions on Pattern Analysis and Machine Intelligence*, 44(12):8766–8778, December 2022. ISSN 1939-3539. doi: 10.1109/tpami.2020.3013679. URL <http://dx.doi.org/10.1109/TPAMI.2020.3013679>.
- Taco Cohen and Max Welling. Group equivariant convolutional networks. In Maria Florina Balcan and Kilian Q. Weinberger, editors, *Proceedings of The 33rd International Conference on Machine Learning*, volume 48 of *Proceedings of Machine Learning Research*, pages 2990–2999, New York, New York, USA, 20–22 Jun 2016. PMLR. URL <https://proceedings.mlr.press/v48/cohen16.html>.
- Taco Cohen, Maurice Weiler, Berkay Kicanaoglu, and Max Welling. Gauge equivariant convolutional networks and the icosahedral cnn. In *International conference on Machine learning*, pages 1321–1330. PMLR, 2019a.
- Taco Cohen et al. *Equivariant convolutional networks*. PhD thesis, Taco Cohen, 2021.
- Taco S. Cohen and Max Welling. Steerable CNNs. In *International Conference on Learning Representations*, 2017. URL <https://openreview.net/forum?id=rJQKYt5H>.
- Taco S Cohen, Mario Geiger, and Maurice Weiler. A general theory of equivariant cnns on homogeneous spaces. *Advances in neural information processing systems*, 32, 2019b.
- Biwei Dai and Uroš Seljak. Translation and rotation equivariant normalizing flow (trenf) for optimal cosmological analysis. 2022. URL <https://doi.org/10.1093/mnras/stac2010>.
- James Damon and J. S. Marron. Backwards Principal Component Analysis and Principal Nested Relations. *Journal of Mathematical Imaging and Vision*, 50(1-2):107–114, October 2013. ISSN 0924-9907, 1573-7683. doi: 10.1007/s10851-013-0463-2. URL <http://link.springer.com/article/10.1007/s10851-013-0463-2>.
- Tim R. Davidson, Luca Falorsi, Nicola De Cao, Thomas Kipf, and Jakub M. Tomczak. Hyperspherical variational auto-encoders. *34th Conference on Uncertainty in Artificial Intelligence 2018, UAI 2018*, 2:856–865, 2018.
- Brad C. Davis, P. Thomas Fletcher, Elizabeth Bullitt, and Sarang Joshi. Population shape regression from random design data. *International Journal of Computer Vision*, 90(2):255–266, jul 2010. ISSN 1573-1405. doi: 10.1007/s11263-010-0367-1. URL <http://dx.doi.org/10.1007/s11263-010-0367-1>.
- Austin Derrow-Pinion, Jennifer She, David Wong, Oliver Lange, Todd Hester, Luis Perez, Marc Nunkesser, Seongjae Lee, Xueying Guo, Brett Wiltshire, Peter W. Battaglia, Vishal Gupta, Ang Li, Zhongwen Xu, Alvaro Sanchez-Gonzalez, Yujia Li, and Petar Velickovic. Eta prediction with graph neural networks in google maps. In *Proceedings of the 30th ACM International Conference on Information & Knowledge Management, CIKM '21*. ACM, October 2021. doi: 10.1145/3459637.3481916. URL <http://dx.doi.org/10.1145/3459637.3481916>.
- Gage DeZoort, Peter W Battaglia, Catherine Biscarat, and Jean-Roch Vlimant. Graph neural networks at the large hadron collider. *Nature Reviews Physics*, 5(5):281–303, 2023.
- Kaize Ding, Jianling Wang, Jundong Li, Dingcheng Li, and Huan Liu. Be more with less: Hypergraph attention networks for inductive text classification. In *Conference on Empirical Methods in Natural Language Processing*, 2020. URL <https://api.semanticscholar.org/CorpusID:226226607>.
- Claire Donnat, Axel Levy, Frederic Poitevin, Ellen Zhong, and Nina Miolane. Deep generative modeling for volume reconstruction in cryo-electron microscopy, 2022.
- Alexey Dosovitskiy, Lucas Beyer, Alexander Kolesnikov, Dirk Weissenborn, Xiaohua Zhai, Thomas Unterthiner, Mostafa Dehghani, Matthias Minderer, Georg Heigold, Sylvain Gelly, Jakob Uszkoreit, and Neil Houlsby. An image is worth 16x16 words: Transformers for image recognition at scale, 2021.
- Stefania Ebli, Michaël Defferrard, and Gard Spreemann. Simplicial neural networks. In *TDA & Beyond*, 2020. URL <https://openreview.net/forum?id=nPCT39DVIfk>.
- Floor Eijkelboom, Rob Hesselink, and Erik J Bekkers. E ( $n$ ) equivariant message passing simplicial networks. In *International Conference on Machine Learning*, pages 9071–9081. PMLR, 2023.
- Nico Engel, Vasileios Belagiannis, and Klaus C. J. Dietmayer. Point transformer. *IEEE Access*, 9:134826–134840, 2020. URL <https://api.semanticscholar.org/CorpusID:226227046>.
- Luca Falorsi, Pim de Haan, Tim R. Davidson, Nicola De Cao, Maurice Weiler, Patrick Forré, and Taco S. Cohen. Explorations in Homeomorphic Variational Auto-Encoding. 2018. URL <http://arxiv.org/abs/1807.04689>.
- Jianqing Fan. Local linear regression smoothers and their minimax efficiencies. *The Annals of Statistics*, 21(1), March 1993. ISSN 0090-5364. doi: 10.1214/aos/1176349022. URL <http://dx.doi.org/10.1214/aos/1176349022>.
- Matthias Fey and Jan E. Lenssen. Fast graph representation learning with PyTorch Geometric. In *ICLR Workshop on Representation Learning on Graphs and Manifolds*, 2019.
- Marc Finzi, Max Welling, and Andrew Gordon Gordon Wilson. A practical method for constructing equivariant multilayer perceptrons for arbitrary matrix groups. In Marina Meila and Tong Zhang, editors, *Proceedings of the 38th International Conference on Machine Learning*, volume 139 of *Proceedings of Machine Learning Research*, pages 3318–3328. PMLR, 18–24 Jul 2021. URL <https://proceedings.mlr.press/v139/finzi21a.html>.
- R. A. Fisher. The use of multiple measurements in taxonomic problems. *Annals of Eugenics*, 7(7):179–188, 1936.
- P. Thomas Fletcher and Sarang Joshi. Riemannian geometry for the statistical analysis of diffusion tensor data. *Signal Processing*, 87(2):250–262, 2007. ISSN 0165-1684. doi: <https://doi.org/10.1016/j.sigpro.2005.12.018>. URL <https://www.sciencedirect.com/science/article/pii/S0165168406001691>.
- P Thomas Fletcher, Conglin Lu, Stephen M Pizer, and Sarang Joshi. Principal geodesic analysis for the study of nonlinear statistics of shape. *IEEE transactions on medical imaging*, 23(8):995–1005, 2004.
- Thomas Fletcher. Geodesic regression on riemannian manifolds. In *Proceedings of the Third International Workshop on Mathematical Foundations of Computational Anatomy-Geometrical and Statistical Methods for Modelling Biological Shape Variability*, pages 75–86, 2011.
- Fabian Fuchs, Daniel Worrall, Volker Fischer, and Max Welling. Se(3)-transformers: 3d roto-translation equivariant attention networks. In H. Larochelle, M. Ranzato, R. Hadsell, M.F. Balcan, and H. Lin, editors, *Advances in Neural Information Processing Systems*, volume 33, pages 1970–1981. Curran Associates, Inc., 2020. URL [https://proceedings.neurips.cc/paper\\_files/paper/2020/file/15231a7ce4ba789d13b722cc5c955834-Paper.pdf](https://proceedings.neurips.cc/paper_files/paper/2020/file/15231a7ce4ba789d13b722cc5c955834-Paper.pdf).
- Yue Gao, Yifan Feng, Shuyi Ji, and Rongrong Ji. Hgnn: General hypergraph neural networks. *IEEE Transactions on Pattern Analysis and Machine Intelligence*, 2022.
- Thomas Gaudelot, Ben Day, Arian R Jamasb, Jyothish Soman, Cristian Regep, Gertrude Liu, Jeremy B R Hayter, Richard Vickers, Charles Roberts, Jian Tang, David Roblin, Tom L Blundell, Michael M Bronstein, and Jake P Taylor-King. Utilizing graph machine learning within drug discovery and development. 2021. URL <https://doi.org/10.1093/bib/bbab159>.
- F Gay-Balmaz, DD Holm, DM Meier, TS Ratiu, and F-X Vialard. Invariant Higher-Order Variational Problems. *Communications in Mathematical Physics*, 309:413–458, 2012. doi: 10.1007/s00220-011-1313-y. URL <http://dx.doi.org/10.1007/s00220-011-1313-y>.
- Niklas W. A. Gebauer, Michael Gastegger, and Kristof T. Schütt. Symmetry-adapted generation of 3d point sets for the targeted discovery of molecules, 2020.
- Mario Geiger, Tess Smidt, Alby M., Benjamin Kurt Miller, Wouter Boomsma, Bradley Dice, Kostiantyn Lapchevskiy, Maurice Weiler, Michał Tyszkiewicz, Simon Batzner, Dylan Madis-

- etti, Martin Uhrin, Jes Frelsen, Nuri Jung, Sophia Sanborn, Mingjian Wen, Josh Rackers, Marcel Röd, and Michael Bailey. Euclidean neural networks: e3nn, April 2022. URL <https://doi.org/10.5281/zenodo.6459381>.
- J.D. Gergonne. Application de la méthode des moindres carrés à l'interpolation des suites. *Annales des Mathématiques Pures et Appliquées*, 6:242–252, 1815.
- Jeff Gill and Dominik Hangartner. Circular data in political science and how to handle it. *Political Analysis*, 18(3):316–336, 2010. ISSN 1476-4989. doi: 10.1093/pan/mpq009. URL <http://dx.doi.org/10.1093/pan/mpq009>.
- Justin Gilmer, Samuel S. Schoenholz, Patrick F. Riley, Oriol Vinyals, and George E. Dahl. Neural message passing for quantum chemistry. In Doina Precup and Yee Whye Teh, editors, *Proceedings of the 34th International Conference on Machine Learning*, volume 70 of *Proceedings of Machine Learning Research*, pages 1263–1272. PMLR, 06–11 Aug 2017. URL <https://proceedings.mlr.press/v70/gilmer17a.html>.
- Lorenzo Giusti, Claudio Battiloro, Lucia Testa, Paolo Di Lorenzo, Stefania Sardellitti, and Sergio Barbarossa. Cell attention networks. In *2023 International Joint Conference on Neural Networks (IJCNN)*. IEEE, June 2023. doi: 10.1109/ijcnn54540.2023.10191530. URL <http://dx.doi.org/10.1109/IJCNN54540.2023.10191530>.
- Simon Graham, David Epstein, and Nasir Rajpoot. Dense steerable filter cnns for exploiting rotational symmetry in histology images, 2020.
- Chaoyu Guan, Ziwei Zhang, Haoyang Li, Heng Chang, Zeyang Zhang, Yijian Qin, Jiyan Jiang, Xin Wang, and Wenwu Zhu. AutoGL: A library for automated graph learning. In *ICLR 2021 Workshop on Geometrical and Topological Representation Learning*, 2021. URL <https://openreview.net/forum?id=0yHwPLeInDn>.
- Nicolas Guigui, Nina Miolane, Xavier Pennec, et al. Introduction to riemannian geometry and geometric statistics: from basic theory to implementation with geomstats. *Foundations and Trends® in Machine Learning*, 16(3):329–493, 2023.
- Meng-Hao Guo, Jun-Xiong Cai, Zheng-Ning Liu, Tai-Jiang Mu, Ralph R. Martin, and Shi-Min Hu. Pct: Point cloud transformer. *Computational Visual Media*, 7(2):187–199, April 2021. ISSN 2096-0662. doi: 10.1007/s41095-021-0229-5. URL <http://dx.doi.org/10.1007/s41095-021-0229-5>.
- Mengmeng Guo, Jingyong Su, Li Sun, and Guofeng Cao. Statistical regression analysis of functional and shape data. *Journal of Applied Statistics*, 47(1):28–44, September 2019. ISSN 1360-0532. doi: 10.1080/02664763.2019.1669541. URL <http://dx.doi.org/10.1080/02664763.2019.1669541>.
- Saumya Gupta, Xiaoling Hu, James Kaan, Michael Jin, Mutshipay Mpoy, Katherine Chung, Gagandeep Singh, Mary Saltz, Tahsin Kurc, Joel Saltz, Apostolos Tassiopoulos, Prateek Prasanna, and Chao Chen. Learning topological interactions for multi-class medical image segmentation, 2022.
- Mehdi Hadj-Hamou, Marco Lorenzi, Nicholas Ayache, and Xavier Pennec. Longitudinal Analysis of Image Time Series with Diffeomorphic Deformations: A Computational Framework Based on Stationary Velocity Fields. *Frontiers in Neuroscience*, 10, 2016. ISSN 1662-453X. doi: 10.3389/fnins.2016.00236. URL <https://www.frontiersin.org/articles/10.3389/fnins.2016.00236/full>.
- Aric Hagberg, Pieter J Swart, and Daniel A Schult. Exploring network structure, dynamics, and function using networkx. Technical report, Los Alamos National Laboratory (LANL), Los Alamos, NM (United States), 2008.
- Mustafa Hajji, Kyle Istvan, and Ghada Zamzmi. Cell complex neural networks. In *TDA & Beyond*, 2020. URL <https://openreview.net/forum?id=6Tq18ySFpGU>.
- Mustafa Hajji, Ghada Zamzmi, Theodore Papamarkou, Nina Miolane, Aldo Guzmán-Sáenz, Karthikeyan Natesan Ramamurthy, Tolga Birdal, Tamal K Dey, Soham Mukherjee, Shreyas N Samaga, et al. Topological deep learning: Going beyond graph data. 2023a.
- Mustafa Hajji, Ghada Zamzmi, Theodore Papamarkou, Nina Miolane, Aldo Guzmán-Sáenz, Karthikeyan Natesan Ramamurthy, Tolga Birdal, Tamal K. Dey, Soham Mukherjee, Shreyas N. Samaga, Neal Livesay, Robin Walters, Paul Rosen, and Michael T. Schaub. Topological deep learning: Going beyond graph data, 2023b.
- Mustafa Hajji, Mathilde Papillon, Florian Frantzen, Jens Agerberg, Ibrahim AlJabea, Ruben Ballester, Claudio Battiloro, Guillermo Bernárdez, Tolga Birdal, Aiden Brent, Peter Chin, Sergio Escalera, Simone Fiorellino, Odin Hoff Gardaa, Gurusankar Gopalakrishnan, Devendra Govil, Josef Hoppe, Manneel Reddy Karri, Jude Khouja, Manuel Lecha, Neal Livesay, Jan Meißner, Soham Mukherjee, Alexander Nikitin, Theodore Papamarkou, Jaro Prflepok, Karthikeyan Natesan Ramamurthy, Paul Rosen, Aldo Guzmán-Sáenz, Alessandro Salatiello, Shreyas N. Samaga, Simone Scardapane, Michael T. Schaub, Luca Scofano, Indro Spinelli, Lev Telyatnikov, Quang Truong, Robin Walters, Maosheng Yang, Olga Zaghen, Ghada Zamzmi, Ali Zia, and Nina Miolane. Topox: A suite of python packages for machine learning on topological domains, 2024. URL <https://arxiv.org/abs/2402.02441>.
- Elkan F. Halpern. Polynomial regression from a bayesian approach. *Journal of the American Statistical Association*, 68(341):137–143, March 1973. ISSN 1537-274X. doi: 10.1080/01621459.1973.10481352. URL <http://dx.doi.org/10.1080/01621459.1973.10481352>.
- Martin Hanik, Hans-Christian Hege, Anja Hennemuth, and Christoph von Tycowicz. Nonlinear regression on manifolds for shape analysis using intrinsic bézier splines. In *International Conference on Medical Image Computing and Computer-Assisted Intervention*, 2020. URL <https://api.semanticscholar.org/CorpusID:220486926>.
- Trevor Hastie and Werner Stuetzle. Principal Curves. *Journal of the American Statistical Association*, 84(406):502–516, 1989.
- Søren Hauberg. Principal Curves on Riemannian Manifolds. *IEEE Transactions on Pattern Analysis and Machine Intelligence*, 38(9):1915–1921, 2016. ISSN 01628828. doi: 10.1109/TPAMI.2015.2496166.
- Lingshen He, Yiming Dong, Yisen Wang, Dacheng Tao, and Zhouchen Lin. Gauge equivariant transformer. In M. Ranzato, A. Beygelzimer, Y. Dauphin, P.S. Liang, and J. Wortman Vaughan, editors, *Advances in Neural Information Processing Systems*, volume 34, pages 27331–27343. Curran Associates, Inc., 2021. URL [https://proceedings.neurips.cc/paper\\_files/paper/2021/file/e57c6b956a6521b28495f2886ca0977a-Paper.pdf](https://proceedings.neurips.cc/paper_files/paper/2021/file/e57c6b956a6521b28495f2886ca0977a-Paper.pdf).
- Sajjad Heydari and Lorenzo Livi. Message passing neural networks for hypergraphs. In Elias Pimenidis, Plamen Angelov, Chrisina Jayne, Antonios Papaleonidas, and Mehmet Aydin, editors, *Artificial Neural Networks and Machine Learning – ICANN 2022*, pages 583–592, Cham, 2022. Springer Nature Switzerland.
- Jacob Hinkle, Prasanna Muralidharan, P. Fletcher, and Sarang Joshi. Polynomial regression on riemannian manifolds. 7574, 10 2012a. doi: 10.1007/978-3-642-33712-3\_1.
- Jacob Hinkle, Prasanna Muralidharan, P Thomas Fletcher, and Sarang Joshi. Polynomial regression on riemannian manifolds. In *European conference on computer vision*, pages 1–14. Springer, 2012b.
- Emiel Hoogeboom, Victor Garcia Satorras, Clément Vignac, and Max Welling. Equivariant diffusion for molecule generation in 3d, 2022.
- Xiaoling Hu, Li Fuxin, Dimitris Samaras, and Chao Chen. Topology-preserving deep image segmentation, 2019.
- Xiaoling Hu, Yusu Wang, Li Fuxin, Dimitris Samaras, and Chao Chen. Topology-aware segmentation using discrete morse theory, 2021.
- Zhiwu Huang and Luc Van Gool. A Riemannian Network for SPD Matrix Learning. pages 2036–2042, 2016. URL <http://arxiv.org/abs/1608.04233>.
- Stephan Huckemann, Thomas Hotz, and Axel Munk. Intrinsic shape analysis: Geodesic PCA for riemannian manifolds modulo isometric lie group actions. *Statistica Sinica*, 20(1):1–58, 2010. ISSN 10170405.

- Michael J. Hutchinson, Charline Le Lan, Sheheryar Zaidi, Emilien Dupont, Yee Whye Teh, and Hyunjik Kim. Lietransformer: Equivariant self-attention for lie groups. In *International Conference on Machine Learning*, 2020. URL <https://api.semanticscholar.org/CorpusID:229340145>.
- J.B. Ingraham, M. Baranov, and Z. et al. Costello. Illuminating protein space with a programmable generative model. 2023. URL <https://doi.org/10.1038/s41586-023-06728-8>.
- John Ingraham, Vikas Garg, Regina Barzilay, and Tommi Jaakkola. Generative models for graph-based protein design. 2019. URL [https://papers.nips.cc/paper\\_files/paper/2019/hash/f3a4ff4839c56a5f460c88cce3666a2b-Abstract.html](https://papers.nips.cc/paper_files/paper/2019/hash/f3a4ff4839c56a5f460c88cce3666a2b-Abstract.html)
- Kristopher T. Jensen, Ta-Chu Kao, Marco Tripodi, and Guillaume Hennequin. Manifold gplvms for discovering non-euclidean latent structure in neural data. In *Proceedings of the 34th International Conference on Neural Information Processing Systems, NIPS '20*, Red Hook, NY, USA, 2020. Curran Associates Inc. ISBN 9781713829546.
- Jianwen Jiang, Yuxuan Wei, Yifan Feng, Jingxuan Cao, and Yue Gao. Dynamic hypergraph neural networks. In *Proceedings of the Twenty-Eighth International Joint Conference on Artificial Intelligence, IJCAI-2019*. International Joint Conferences on Artificial Intelligence Organization, August 2019. doi: 10.24963/ijcai.2019/366. URL <http://dx.doi.org/10.24963/ijcai.2019/366>.
- Richard A. Johnson and Thomas E. Wehrly. Some angular-linear distributions and related regression models. *Journal of the American Statistical Association*, 73:602–606, 1978. URL <https://api.semanticscholar.org/CorpusID:122640093>.
- J. Jumper, R. Evans, and A. et al. Pritzel. Highly accurate protein structure prediction with alphafold. *Nature*, 2021. URL <https://doi.org/10.1038/s41586-021-03819-2>.
- Seungwoo Kang and Hee-Seok Oh. Probabilistic Principal Curves on Riemannian Manifolds. *IEEE Transactions on Pattern Analysis and Machine Intelligence*, 46(7):4843–4849, July 2024. ISSN 0162-8828, 2160-9292, 1939-3539. doi: 10.1109/TPAMI.2024.3357801. URL <https://ieeexplore.ieee.org/document/10413614/>.
- Ryan Keisler. Forecasting global weather with graph neural networks, 2022.
- Diederik P. Kingma and Max Welling. Auto-Encoding Variational Bayes. In *Proceedings of the 2nd International Conference on Learning Representations (ICLR)*, 2014.
- Thomas N. Kipf and Max Welling. Semi-supervised classification with graph convolutional networks. In *International Conference on Learning Representations*, 2017. URL <https://openreview.net/forum?id=SJU4ayYgl>.
- Max Kochurov, Rasul Karimov, and Serge Kozlukov. Geoopt: Riemannian optimization in pytorch, 2020.
- Dimitrios Konstantinidis, Ilias Papastratis, Kosmas Dimitropoulos, and Petros Daras. Multi-manifold attention for vision transformers. *IEEE Access*, 11:123433–123444, 2023. ISSN 2169-3536. doi: 10.1109/access.2023.3329952. URL <http://dx.doi.org/10.1109/ACCESS.2023.3329952>.
- Nikola Kovachki, Zongyi Li, Burigede Liu, Kamyar Azizzadenesheli, Kaushik Bhattacharya, Andrew Stuart, and Anima Anandkumar. Neural operator: Learning maps between function spaces with applications to pdes. *Journal of Machine Learning Research*, 24(89):1–97, 2023.
- Alex Krizhevsky, Ilya Sutskever, and Geoffrey E. Hinton. ImageNet classification with deep convolutional neural networks. *Communications of the ACM*, 60:84 – 90, 2012. URL <https://api.semanticscholar.org/CorpusID:195908774>.
- Line Kühnel and Stefan Sommer. Stochastic development regression on non-linear manifolds. In *Information Processing in Medical Imaging*, 2017. URL <https://api.semanticscholar.org/CorpusID:122942>.
- Soumyabrata Kundu and Risi Kondor. Steerable transformers. *arXiv preprint arXiv:2405.15932*, 2024.
- Maxime W. Lafarge, Erik J. Bekkers, Josien P. W. Pluim, Remco Duits, and Mitko Veta. Roto-translation equivariant convolutional networks: Application to histopathology image analysis, 2020.
- Remi Lam, Alvaro Sanchez-Gonzalez, Matthew Willson, Peter Wirnsberger, Meire Fortunato, Ferran Alet, Suman Ravuri, Timo Ewalds, Zach Eaton-Rosen, Weihua Hu, Alexander Merose, Stephan Hoyer, George Holland, Oriol Vinyals, Jacklynn Stott, Alexander Pritzel, Shakir Mohamed, and Peter Battaglia. Graphcast: Learning skillful medium-range global weather forecasting, 2023.
- Nicholas W. Landry, Maxime Lucas, Iacopo Iacopini, Giovanni Petri, Alice Schwarze, Alice Patania, and Leo Torres. XGI: A Python package for higher-order interaction networks. *Journal of Open Source Software*, 8(85):5162, May 2023. doi: 10.21105/joss.05162. URL <https://doi.org/10.21105/joss.05162>.
- Neil Lawrence. Gaussian process latent variable models for visualisation of high dimensional data. In S. Thrun, L. Saul, and B. Schölkopf, editors, *Advances in Neural Information Processing Systems*, volume 16. MIT Press, 2003. URL [https://proceedings.neurips.cc/paper\\_files/paper/2003/file/9657c1ffff38824e5ab0472e022e577e-Paper.pdf](https://proceedings.neurips.cc/paper_files/paper/2003/file/9657c1ffff38824e5ab0472e022e577e-Paper.pdf).
- Alice Le Brigant and Stéphane Puechmorel. Optimal Riemannian quantization with an application to air traffic analysis. *arXiv preprint arXiv:1806.07605*, 2018.
- Yann LeCun, Leon Bottou, Yoshua Bengio, and Patrick Haffner. Gradient-Based Learning Applied to Document Recognition. *Proc. of the IEEE*, 86(11):2278 – 2324, 1998.
- Juho Lee, Yoonho Lee, Jungtaek Kim, Adam Kosiosek, Seungjin Choi, and Yee Whye Teh. Set transformer: A framework for attention-based permutation-invariant neural networks. In Kamalika Chaudhuri and Ruslan Salakhutdinov, editors, *Proceedings of the 36th International Conference on Machine Learning*, volume 97 of *Proceedings of Machine Learning Research*, pages 3744–3753. PMLR, 09–15 Jun 2019. URL <https://proceedings.mlr.press/v97/lee19d.html>.
- See Lee, Feng Ji, and Wee Peng Tay. Sgat: Simplicial graph attention network. pages 3167–3175, 07 2022. doi: 10.24963/ijcai.2022/440.
- Adrien-Marie Legendre. Nouvelles méthodes pour la détermination des orbites des comètes. 1805.
- M.M. Li, K. Huang, and M. Zitnik. Graph representation learning in biomedicine and healthcare. *Nature Biomedicine*, 2022a. URL <https://doi.org/10.1038/s41551-022-00942-x>.
- Zhengyu Li, XUAN TANG, Zihao Xu, Xihao Wang, Hui Yu, Mingsong Chen, and xian wei. Geodesic self-attention for 3d point clouds. In S. Koyejo, S. Mohamed, A. Agarwal, D. Belgrave, K. Cho, and A. Oh, editors, *Advances in Neural Information Processing Systems*, volume 35, pages 6190–6203. Curran Associates, Inc., 2022b. URL [https://proceedings.neurips.cc/paper\\_files/paper/2022/file/28e4ee96c94e31b2d040b4521d2b299e-Paper-Conference.pdf](https://proceedings.neurips.cc/paper_files/paper/2022/file/28e4ee96c94e31b2d040b4521d2b299e-Paper-Conference.pdf).
- Lizhen Lin, Brian St. Thomas, Hongtu Zhu, and David B. Dunson. Extrinsic local regression on manifold-valued data. *Journal of the American Statistical Association*, 112(519):1261–1273, May 2017. ISSN 1537-274X. doi: 10.1080/01621459.2016.1208615. URL <http://dx.doi.org/10.1080/01621459.2016.1208615>.
- Cong Liu, David Ruhe, Floor Eijkelboom, and Patrick Forré. Clifford group equivariant simplicial message passing networks. *arXiv preprint arXiv:2402.10011*, 2024.
- Meng Liu, Youzhi Luo, Limei Wang, Yaochen Xie, Haonan Yuan, Shurui Gui, Zhao Xu, Haiyang Yu, Jingtun Zhang, Yi Liu, Keqiang Yan, Bora Oztekin, Haoran Liu, Xuan Zhang, Cong Fu, and Shuiwang Ji. Dig: A turnkey library for diving into graph deep learning research. *ArXiv*, abs/2103.12608, 2021. URL <https://api.semanticscholar.org/CorpusID:232320529>.
- Francesco Locatello, Dirk Weissenborn, Thomas Unterthiner, Aravindh Mahendran, Georg Heigold, Jakob Uszkoreit, Alexey Dosovitskiy, and Thomas Kipf. Object-centric learning with slot attention, 2020.
- Marco Lorenzi and Xavier Pennec. Geodesics, Parallel Transport & One-parameter Subgroups for Diffeomorphic Image Registration. *International Journal of Computer Vision*, 105(2):111–127, November 2013. doi: 10.1007/s11263-012-0598-4. URL

- <https://hal.inria.fr/hal-00813835>. Publisher: Springer Verlag.
- Marco Lorenzi, Xavier Pennec, Giovanni B. Frisoni, and Nicholas Ayache. Disentangling normal aging from Alzheimer’s disease in structural magnetic resonance images. *Neurobiology of Aging*, 36:S42–S52, January 2015. ISSN 01974580. doi: 10.1016/j.neurobiolaging.2014.07.046. URL <https://linkinghub.elsevier.com/retrieve/pii/S0197458014005594>.
- Youzhi Luo and Shuiwang Ji. An autoregressive flow model for 3d molecular geometry generation from scratch. In *International Conference on Learning Representations*, 2022. URL <https://api.semanticscholar.org/CorpusID:251647192>.
- L. Machado, F. Silva Leite, and K. Krakowski. Higher-order smoothing splines versus least squares problems on Riemannian manifolds. *Journal of Dynamical and Control Systems*, 16(1):121–148, January 2010. ISSN 1079-2724, 1573-8698. doi: 10.1007/s10883-010-9080-1. URL <http://link.springer.com/10.1007/s10883-010-9080-1>.
- Luis Machado and F Silva Leite. Fitting Smooth Paths on Riemannian Manifolds. *International Journal of Applied Mathematics and Statistics*, 4, 2006.
- Elodie Maignant, Alain Trouvé, and Xavier Pennec. *Riemannian Locally Linear Embedding with Application to Kendall Shape Spaces*, page 12–20. Springer Nature Switzerland, 2023. ISBN 9783031382710. doi: 10.1007/978-3-031-38271-0\_2. URL [http://dx.doi.org/10.1007/978-3-031-38271-0\\_2](http://dx.doi.org/10.1007/978-3-031-38271-0_2).
- Anton Mallasto and Aasa Feragen. Application de la methode des moindres quares a l’interpolation des suites. In *Annales des Math Pures*, pages 5580–5588, 2018.
- Jason D. McEwen, Christopher G. R. Wallis, and Augustine N. Mavor-Parker. Scattering networks on the sphere for scalable and rotationally equivariant spherical cnns, 2022.
- Leland McInnes, John Healy, Nathaniel Saul, and Lukas Großberger. Umap: Uniform manifold approximation and projection. *Journal of Open Source Software*, 3(29):861, 2018. doi: 10.21105/joss.00861. URL <https://doi.org/10.21105/joss.00861>.
- Maciej Mikulski and Jaroslaw Duda. Toroidal autoencoder, 2019.
- N. Miolane and X. Pennec. Computing bi-invariant pseudo-metrics on lie groups for consistent statistics. *Entropy*, 17(4), 2015. ISSN 10994300. doi: 10.3390/e17041850.
- N. Miolane, A. Le Brigant, B. Hou, C. Donnat, M. Jorda, J. Mathe, X. Pennec, and S. Holmes. Geomstats: a python module for computations and statistics on manifolds. *Submitted to JMLR*, 2019. URL <https://github.com/geomstats/geomstats>.
- Nina Miolane and Susan Holmes. Learning weighted submanifolds with variational autoencoders and riemannian variational autoencoders. In *Proceedings of the IEEE/CVF Conference on Computer Vision and Pattern Recognition*, pages 14503–14511, 2020.
- Nina Miolane, Frederic Poitevin, Yee-Ting Li, and Susan Holmes. Estimation of orientation and camera parameters from cryo-electron microscopy images with variational autoencoders and generative adversarial networks. In *Proceedings of the IEEE/CVF Conference on Computer Vision and Pattern Recognition (CVPR) Workshops*, June 2020.
- Prasanna Muralidharan, Jacob Hinkle, and P. Fletcher. A map estimation algorithm for bayesian polynomial regression on riemannian manifolds. pages 215–219, 09 2017. doi: 10.1109/ICIP.2017.8296274.
- E. A. Nadaraya. On estimating regression. *Theory of Probability and its Applications*, 9:141–142, 1964.
- Maximillian Nickel and Douwe Kiela. Poincaré embeddings for learning hierarchical representations. *Advances in neural information processing systems*, 30, 2017.
- Victor M. Panaretos, Tung Pham, and Zhigang Yao. Principal flows. *Journal of the American Statistical Association*, 109(505): 424–436, 2014. ISSN 1537274X. doi: 10.1080/01621459.2013.849199.
- Mathilde Papillon, Sophia Sanborn, Mustafa Hajj, and Nina Miolane. Architectures of topological deep learning: A survey on topological neural networks. *arXiv preprint arXiv:2304.10031*, 2023.
- Karl Pearson. Liii. on lines and planes of closest fit to systems of points in space. *The London, Edinburgh, and Dublin philosophical magazine and journal of science*, 2(11):559–572, 1901.
- Bruno Pelletier. Non-parametric regression estimation on closed riemannian manifolds. *Journal of Nonparametric Statistics*, 18:57 – 67, 2006. URL <https://api.semanticscholar.org/CorpusID:17937994>.
- X. Pennec, S. Sommer, and T. Fletcher. *Riemannian Geometric Statistics in Medical Image Analysis*. Elsevier Science & Technology, 2019. ISBN 978-0-12-814725-2. URL <https://books.google.com/books?id=k8qsDwAAQBAJ>.
- Xavier Pennec. Intrinsic Statistics on Riemannian Manifolds: Basic Tools for Geometric Measurements. *Journal of Mathematical Imaging and Vision*, 25(1):127–154, 2006. ISSN 0924-9907.
- Xavier Pennec. Barycentric subspace analysis on manifolds. *Annals of Statistics*, 46(6A):2711–2746, 2018. ISSN 00905364. doi: 10.1214/17-AOS1636.
- Xavier Pennec and Vincent Arsigny. Exponential Barycenters of the Canonical Cartan Connection and Invariant Means on Lie Groups. In Frederic Barbaresco, Amit Mishra, and Frank Nielsen, editors, *Matrix Information Geometry*, pages 123–168. Springer, 5 2012. ISBN 978-3-642-30231-2 (Print) / 978-3-642-30232-9 (Online). doi: 10.1007/978-3-642-30232-9.
- Xavier Pennec and Marco Lorenzi. 5 - Beyond Riemannian geometry: The affine connection setting for transformation groups. In Xavier Pennec, Stefan Sommer, and Tom Fletcher, editors, *Riemannian Geometric Statistics in Medical Image Analysis*, pages 169–229. Academic Press, January 2020. ISBN 978-0-12-814725-2. doi: 10.1016/B978-0-12-814725-2.00012-1. URL <http://www.sciencedirect.com/science/article/pii/B9780128147252000121>.
- Xavier Pennec and Jean-Philippe Thirion. A Framework for Uncertainty and Validation of 3D Registration Methods based on Points and Frames. *Int. Journal of Computer Vision*, 25(3): 203–229, December 1997. doi: 10.1023/A:1007976002485. URL <http://www.springerlink.com/openurl.asp?genre=article&issn=0920-5691&volume=25&issn=0920-5691>.
- Xavier Pennec, Pierre Fillard, and Nicholas Ayache. A Riemannian Framework for Tensor Computing. *International Journal of Computer Vision*, 66(1):41–66, 1 2006.
- Alexander Petersen and Hans-Georg Muller. Fréchet regression for random objects with euclidean predictors. *The Annals of Statistics*, 2016. URL <https://api.semanticscholar.org/CorpusID:13666043>.
- Tobias Pfaff, Meire Fortunato, Alvaro Sanchez-Gonzalez, and Peter W. Battaglia. Learning mesh-based simulation with graph networks, 2021.
- Stephen M. Pizer, P. Thomas Fletcher, Sarang Joshi, Andrew Thall, Jiahui Z. Chen, Yael Fridman, Daniel S. Fritsch, Grant Gash, James M. Glotzer, Mark R. Jiroutek, Chiu Lu, Keith E. Muller, George Tracton, Paul Yushkevich, and Edward L. Chaney. Deformable m-reps for 3d medical image segmentation. *International Journal of Computer Vision*, 55(2-3):85–106, November 2003. doi: 10.1023/a:1026313132218.
- Brenda Praggastis, Sinan G. Aksoy, Dustin Arendt, Mark Bonicillo, Cliff A Joslyn, Emilie Purvine, Madelyn R Shapiro, and Ji Young Yun. Hypernetx: A python package for modeling complex network data as hypergraphs. *ArXiv*, abs/2310.11626, 2023. URL <https://api.semanticscholar.org/CorpusID:264288882>.
- PyT-Team. Topobenchmarkx, 2024.
- Charles Ruizhongtai Qi, Li Yi, Hao Su, and Leonidas J Guibas. Pointnet++: Deep hierarchical feature learning on point sets in a metric space. In I. Guyon, U. Von Luxburg, S. Bengio, H. Wallach, R. Fergus, S. Vishwanathan, and R. Garnett, editors, *Advances in Neural Information Processing Systems*, volume 30. Curran Associates, Inc., 2017. URL [https://proceedings.neurips.cc/paper\\_files/paper/2017/file/d8bf84be3800d12f74d8b05e9b89836f-Paper.pdf](https://proceedings.neurips.cc/paper_files/paper/2017/file/d8bf84be3800d12f74d8b05e9b89836f-Paper.pdf).
- P. Rajpurkar, E. Chen, and O. et al. Banerjee. Ai in health and medicine. *Nature Medicine*, 2022. URL <https://doi.org/10.1038/s41591-021-01614-0>.
- Danny Reidenbach and Aditi S. Krishnapriyan. Coarsenconf:

- Equivariant coarsening with aggregated attention for molecular conformer generation, 2023.
- P. Reiser, M. Neubert, and A. et al. Eberhard. Graph neural networks for materials science and chemistry. 2022. URL <https://doi.org/10.1038/s43246-022-00315-6>.
- T. Mitchell Roddenberry, Michael T. Schaub, and Mustafa Hajj. Signal processing on cell complexes. In *ICASSP 2022 - 2022 IEEE International Conference on Acoustics, Speech and Signal Processing (ICASSP)*, pages 8852–8856, 2022. doi: 10.1109/ICASSP43922.2022.9747233.
- Frank Rosenblatt. The perceptron: a probabilistic model for information storage and organization in the brain. *Psychological review*, 65(6):386, 1958.
- Sam T. Roweis and Lawrence K. Saul. Nonlinear Dimensionality Reduction by Locally Linear Embedding. *Science*, 290(22):2323–2326, 2000. URL <http://www.robots.ox.ac.uk/~az/lectures/ml/llc.pdf>.
- David E. Rumelhart, Geoffrey E. Hinton, and Ronald J. Williams. Learning representations by back-propagating errors. *Nature*, 323:533–536, 1986. URL <https://api.semanticscholar.org/CorpusID:205001834>.
- Alvaro Sanchez-Gonzalez, Jonathan Godwin, Tobias Pfaff, Rex Ying, Jure Leskovec, and Peter W. Battaglia. Learning to simulate complex physics with graph networks, 2020.
- Victor Garcia Satorras, Emiel Hoogeboom, and Max Welling. E(n) equivariant graph neural networks. In *International conference on machine learning*, pages 9323–9332. PMLR, 2021.
- Victor Garcia Satorras, Emiel Hoogeboom, and Max Welling. E(n) equivariant graph neural networks, 2022.
- Anna M M Scaife and Fiona Porter. Fanaroff–riley classification of radio galaxies using group-equivariant convolutional neural networks. *Monthly Notices of the Royal Astronomical Society*, 503(2):2369–2379, February 2021. ISSN 1365-2966. doi: 10.1093/mnras/stab530. URL <http://dx.doi.org/10.1093/mnras/stab530>.
- Christof Schötz. Nonparametric regression in nonstandard spaces. *Electronic Journal of Statistics*, 16(2):4679 – 4741, 2022. doi: 10.1214/22-EJS2056. URL <https://doi.org/10.1214/22-EJS2056>.
- Kristof T. Schütt, Pieter-Jan Kindermans, Huziel E. Sauceda, Stefan Chmiela, Alexandre Tkatchenko, and Klaus-Robert Müller. SchNet: A continuous-filter convolutional neural network for modeling quantum interactions, 2017.
- Xiaoyan Shi, Martin Styner, Jeffrey Lieberman, Joseph G. Ibrahim, Weili Lin, and Hongtu Zhu. *Intrinsic Regression Models for Manifold-Valued Data*, page 192–199. Springer Berlin Heidelberg, 2009. ISBN 9783642042713. doi: 10.1007/978-3-642-04271-3\_24. URL [http://dx.doi.org/10.1007/978-3-642-04271-3\\_24](http://dx.doi.org/10.1007/978-3-642-04271-3_24).
- Gregor N. C. Simm, Robert Pinsler, Gábor Csányi, and José Miguel Hernández-Lobato. Symmetry-aware actor-critic for 3d molecular design, 2020.
- Martin Simonovsky and Nikos Komodakis. Graphvae: Towards generation of small graphs using variational autoencoders, 2018.
- Raphaël Sivera, Hervé Delingette, Marco Lorenzi, Xavier Pennec, and Nicholas Ayache. A model of brain morphological changes related to aging and Alzheimer’s disease from cross-sectional assessments. *NeuroImage*, 198:255–270, September 2019. ISSN 10538119. doi: 10.1016/j.neuroimage.2019.05.040. URL <https://linkinghub.elsevier.com/retrieve/pii/S105381191930432X>.
- Stefan Sommer. Horizontal Dimensionality Reduction and Iterated Frame Bundle Development. In Frank Nielsen and Frédéric Barbaresco, editors, *Geometric Science of Information*, pages 76–83. Springer Berlin Heidelberg, 2013. ISBN 978-3-642-40019-3 978-3-642-40020-9. URL [http://link.springer.com/chapter/10.1007/978-3-642-40020-9\\_7](http://link.springer.com/chapter/10.1007/978-3-642-40020-9_7).
- Stefan Sommer, François Lauze, and Mads Nielsen. Optimization over geodesics for exact principal geodesic analysis. *Advances in Computational Mathematics*, 40(2):283–313, 2014.
- Florian Steinke, Matthias Hein, Jan Peters, and Bernhard Schölkopf. Manifold-valued thin-plate splines with applications in computer graphics. *Comput. Graph. Forum*, 27:437–448, 04 2008. doi: 10.1111/j.1467-8659.2008.01141.x.
- Jonathan M Stokes, Kevin Yang, Kyle Swanson, Wengong Jin, Andres Cubillos-Ruiz, Nina M. Donghia, Craig R. MacNair, Shawn French, Lindsey A. Carfrae, Zohar Bloom-Ackermann, Victoria M. Tran, Anush Chiappino-Pepe, Ahmed H. Badran, Ian W. Andrews, Emma J. Chory, George Church, Eric D. Brown, T. Jaakkola, Regina Barzilay, and James J Collins. A deep learning approach to antibiotic discovery. *Cell*, 180:688–702.e13, 2020. URL <https://api.semanticscholar.org/CorpusID:261621991>.
- Joshua B. Tenenbaum, Vin de Silva, and John C. Langford. A Global Geometric Framework for Nonlinear Dimensionality Reduction. *Science*, 290(5500):2319, 2000.
- Nathaniel Thomas, Tess Smidt, Steven Kearnes, Lusann Yang, Li Li, Kai Kohlhoff, and Patrick Riley. Tensor field networks: Rotation- and translation-equivariant neural networks for 3D point clouds. 2018. URL <http://arxiv.org/abs/1802.08219>.
- Michael E Tipping and Christopher M Bishop. Probabilistic principal component analysis. *Journal of the Royal Statistical Society: Series B (Statistical Methodology)*, 61(3):611–622, 1999.
- James Townsend, Niklas Koep, and Sebastian Weichwald. Pymanopt: A python toolbox for optimization on manifolds using automatic differentiation. *J. Mach. Learn. Res.*, 17:137:1–137:5, 2016. URL <https://api.semanticscholar.org/CorpusID:29194288>.
- Alain Trounev. Diffeomorphisms Groups and Pattern Matching in Image Analysis. *International Journal of Computer Vision*, 28(3):213–221, 1998. ISSN 1573-1405.
- Dimosthenis Tsagkraloulis and Giovanni Montana. Random forest regression for manifold-valued responses. *Pattern Recognition Letters*, 101:6–13, January 2018. ISSN 0167-8655. doi: 10.1016/j.patrec.2017.11.008. URL <http://dx.doi.org/10.1016/j.patrec.2017.11.008>.
- Laurens van der Maaten and Geoffrey Hinton. Visualizing Data using {t-SNE}. *Journal of Machine Learning Research*, 9:2579–2605, 2008.
- Ashish Vaswani, Noam Shazeer, Niki Parmar, Jakob Uszkoreit, Llion Jones, Aidan N Gomez, Łukasz Kaiser, and Illia Polosukhin. Attention is all you need. In I. Guyon, U. Von Luxburg, S. Bengio, H. Wallach, R. Fergus, S. Vishwanathan, and R. Garnett, editors, *Advances in Neural Information Processing Systems*, volume 30. Curran Associates, Inc., 2017. URL [https://proceedings.neurips.cc/paper\\_files/paper/2017/file/3f5ee243547dee91fbd053c1c4a845aa-Paper.pdf](https://proceedings.neurips.cc/paper_files/paper/2017/file/3f5ee243547dee91fbd053c1c4a845aa-Paper.pdf).
- Bastiaan S. Veeling, Jasper Linmans, Jim Winkens, Taco Cohen, and Max Welling. Rotation equivariant cnns for digital pathology, 2018.
- Petar Veličković, Guillem Cucurull, Arantxa Casanova, Adriana Romero, Pietro Liò, and Yoshua Bengio. Graph Attention Networks. *International Conference on Learning Representations*, 2018. URL <https://openreview.net/forum?id=JXMPikCZ>.
- Clement Vignac, Nagham Osman, Laura Toni, and Pascal Frossard. Midi: Mixed graph and 3d denoising diffusion for molecule generation, 2023.
- Hanchen Wang, Tianfan Fu, Yuanqi Du, Wenhao Gao, Kexin Huang, Ziming Liu, Payal Chandak, Shengchao Liu, Peter Van Katwyk, Andreea Deac, Anima Anandkumar, Karianne J. Bergen, Carla P. Gomes, Shirley Ho, Pushmeet Kohli, Joan Lasenby, Jure Leskovec, Tie-Yan Liu, Arjun K. Manrai, Debora S. Marks, Bharath Ramsundar, Le Song, Jimeng Sun, Jian Tang, Petar Velickovic, Max Welling, Linfeng Zhang, Connor W. Coley, Yoshua Bengio, and Marinka Zitnik. Scientific discovery in the age of artificial intelligence. *Nature*, 620:47–60, 2023. URL <https://api.semanticscholar.org/CorpusID:260384616>.
- Minjie Wang, Da Zheng, Zihao Ye, Quan Gan, Mufei Li, Xiang Song, Jinjing Zhou, Chao Ma, Lingfan Yu, Yu Gai, Tianjun Xiao, Tong He, George Karypis, Jinyang Li, and Zheng Zhang. Deep graph library: A graph-centric, highly-performant package for graph neural networks. *arXiv preprint arXiv:1909.01315*, 2019.
- Minmin Wang. Height and diameter of brownian tree. *Electronic Communications in Probability*, 20(none), January 2015. ISSN 1083-589X. doi: 10.1214/ecp.v20-4193. URL

- <http://dx.doi.org/10.1214/ECP.v20-4193>.
- Maurice Weiler et al. Equivariant and coordinate independent convolutional networks: A gauge field theory of neural networks. 2024.
- Christopher Williams and Carl Rasmussen. Gaussian processes for regression. In D. Touretzky, M.C. Mozer, and M. Hasselmo, editors, *Advances in Neural Information Processing Systems*, volume 8. MIT Press, 1995. URL [https://proceedings.neurips.cc/paper\\_files/paper/1995/file/7cce53cf90577442771720a370c3c723-Paper.pdf](https://proceedings.neurips.cc/paper_files/paper/1995/file/7cce53cf90577442771720a370c3c723-Paper.pdf).
- Shiwen Wu, Fei Sun, Wentao Zhang, Xu Xie, and Bin Cui. Graph neural networks in recommender systems: A survey. *ACM Comput. Surv.*, 55(5), dec 2022. ISSN 0360-0300. doi: 10.1145/3535101. URL <https://doi.org/10.1145/3535101>.
- Zonghan Wu, Shirui Pan, Fengwen Chen, Guodong Long, Chengqi Zhang, and Philip S. Yu. A comprehensive survey on graph neural networks. *IEEE Transactions on Neural Networks and Learning Systems*, 32(1):4–24, 2021. doi: 10.1109/TNNLS.2020.2978386.
- Minkai Xu, Lantao Yu, Yang Song, Chence Shi, Stefano Ermon, and Jian Tang. Geodiff: a geometric diffusion model for molecular conformation generation, 2022.
- Minkai Xu, Alexander Powers, Ron Dror, Stefano Ermon, and Jure Leskovec. Geometric latent diffusion models for 3d molecule generation, 2023.
- Yun Yang and David B. Dunson. Bayesian manifold regression. *The Annals of Statistics*, 44(2):876 – 905, 2016. doi: 10.1214/15-AOS1390. URL <https://doi.org/10.1214/15-AOS1390>.
- Z. Yang, X. Zeng, and Y. et al. Zhao. Alphafold2 and its applications in the fields of biology and medicine. 2023. URL <https://doi.org/10.1038/s41392-023-01381-z>.
- Rex Ying, Ruining He, Kaifeng Chen, Pong Eksombatchai, William L. Hamilton, and Jure Leskovec. Graph convolutional neural networks for web-scale recommender systems. In *Proceedings of the 24th ACM SIGKDD International Conference on Knowledge Discovery & Data Mining, KDD '18*. ACM, July 2018. doi: 10.1145/3219819.3219890. URL <http://dx.doi.org/10.1145/3219819.3219890>.
- Laurent Younes. *Shapes and diffeomorphisms*. Number v. 171 in Applied mathematical sciences. Springer, Heidelberg ; New York, 2010. ISBN 978-3-642-12054-1. OCLC: ocn632088149.
- Liangliang Zhang, Yushu Shi, Robert R. Jenq, Kim-Anh Do, and Christine B. Peterson. Bayesian compositional regression with structured priors for microbiome feature selection. *Biometrics*, 77(3):824–838, July 2020. ISSN 1541-0420. doi: 10.1111/biom.13335. URL <http://dx.doi.org/10.1111/biom.13335>.
- Miaomiao Zhang and P. Thomas Fletcher. Probabilistic principal geodesic analysis. *Advances in Neural Information Processing Systems*, pages 1–9, 2013. ISSN 10495258.